© 2016. Published by The Company of Biologists Ltd | Development (2016) 143, 2135-2146 doi:10.1242/dev.132019

RESEARCH ARTICLE

Identification of a regulatory domain controlling the *Nppa-Nppb* gene cluster during heart development and stress

Irina A. Sergeeva[1], Ingeborg B. Hooijkaas[1], Jan M. Ruijter[1], Ingeborg van der Made[2], Nina E. de Groot[2], Harmen J. G. van de Werken[3], Esther E. Creemers[2] and Vincent M. Christoffels[1,*]

ABSTRACT

The paralogous genes *Nppa* and *Nppb* are organized in an evolutionarily conserved cluster and provide a valuable model for studying co-regulation and regulatory landscape organization during heart development and disease. Here, we analyzed the chromatin conformation, epigenetic status and enhancer potential of sequences of the *Nppa-Nppb* cluster *in vivo*. Our data indicate that the regulatory landscape of the cluster is present within a 60-kb domain centered around *Nppb*. Both promoters and several potential regulatory elements interact with each other in a similar manner in different tissues and developmental stages. The distribution of H3K27ac and the association of Pol2 across the locus changed during cardiac hypertrophy, revealing their potential involvement in stress-mediated gene regulation. Functional analysis of double-reporter transgenic mice revealed that *Nppa* and *Nppb* share developmental, but not stress-response, enhancers, responsible for their co-regulation. Moreover, the *Nppb* promoter was required, but not sufficient, for hypertrophy-induced *Nppa* expression. In summary, the developmental regulation and stress response of the *Nppa-Nppb* cluster involve the concerted action of multiple enhancers and epigenetic changes distributed across a structurally rigid regulatory domain.

KEY WORDS: Atrial and brain natriuretic peptide, Chromosome conformation, Epigenetics, Heart development, Hypertrophy, Mouse

INTRODUCTION

Cell type-specific gene expression is regulated through regulatory DNA elements such as enhancers and repressors that function in strictly context-dependent manners. This context includes sequence- and epigenetic signature-dependent binding of complexes of transcription factors and co-factors at selective locations in the DNA and the three-dimensional (3D) conformation of the chromatin that brings these locations together. There is a paucity in the understanding of these mechanisms as only a few regulatory elements have been identified that drive gene expression during development and under pathological conditions *in vivo* (Kathiriya et al., 2015; de Laat and Duboule, 2013; Sanyal et al., 2012). To gain insight into these mechanisms, we studied the regulation of the *Nppa-Nppb* gene cluster during cardiac development and hypertrophy.

[1]Department of Anatomy, Embryology and Physiology, Academic Medical Center, Meibergdreef 9, Amsterdam 1105 AZ, The Netherlands. [2]Department of Experimental Cardiology, Heart Failure Research Center, Academic Medical Center, Meibergdreef 9, Amsterdam 1105 AZ, The Netherlands. [3]Cancer Computational Biology Center, Wytemaweg 80, Erasmus MC Cancer Institute, Erasmus MC, Rotterdam 3015 CN, The Netherlands.

*Author for correspondence (v.m.christoffels@amc.uva.nl)

Received 21 October 2015; Accepted 29 March 2016

In the embryo, natriuretic peptide type A (also known as atrial natriuretic factor, ANF) and type B (also known as brain natriuretic peptide, BNP), encoded by *Nppa* and *Nppb*, respectively, are expressed in the atrial and ventricular myocardium. Both genes are also expressed in the adult heart (Cameron et al., 1996; Houweling et al., 2005) but *Nppa* is downregulated in the ventricles around birth to become restricted to the atria and the ventricular conduction system (Moorman and Christoffels, 2003). Both genes are strongly induced in the ventricles by stress and heart failure, and have become reliable clinical and experimental biomarkers for the severity of hypertrophy and heart failure (Guo et al., 2011; Sergeeva et al., 2014; Troughton et al., 2014). Moreover, *Nppa* is an important marker of early developmental malformations leading to congenital heart defects (Bruneau, 2011). Although the clinical relevance of *Nppa* and *Nppb* expression has led to studies on the regulation of *Nppa* and *Nppb* expression, the understanding of this complex process is still very limited.

Nppa and *Nppb* have descended from an ancestral CNP-3 gene by duplication and variation (Inoue et al., 2003). They are positioned at 10 to 15 kb distance from each other in the mammalian genome. Analysis of other gene clusters, such as Iroquois and Hox, revealed that multiple genes within a cluster have similar expression patterns and are regulated by shared regulatory sequences (Nolte et al., 2013; Tena et al., 2011). These features may underlie the evolutionary stability of such clusters. Therefore, we hypothesize that *Nppa* and *Nppb* are co-regulated by shared regulatory elements and transcriptional mechanisms.

Previously, it has been shown that the proximal *Nppa* promoter responded to stress *in vitro* but not *in vivo* (Knowlton et al., 1995), suggesting involvement of distal regulatory elements required for stress-induced *Nppa* expression. The region spanning from −141 kb to +58 kb relative to *Nppa* contains the transcriptional control information sufficient for both the developmental expression pattern and stress response of *Nppa* and *Nppb* (Sergeeva et al., 2014). Several regulatory elements located 20-37 kb upstream of *Nppa* were able to drive *Nppa*-like expression patterns during development (Matsuoka et al., 2014; Warren et al., 2011). One fragment induced reporter gene reactivation during cardiac hypertrophy. However, this fragment is located outside the −27/+58 kb region sufficient for the *Nppa* stress response (Horsthuis et al., 2008). The promoter regions of human (Majalahti et al., 2007), rat (He et al., 2001) and mouse (V.M.C., unpublished observations) *Nppb* in transgenic mice showed only very limited capacities to drive reporter expression in the normal and the stressed heart, and the developmental activity of these regions has not been described. Therefore, we have an incomplete understanding of the coordinated action of developmental and stress-induced regulatory elements.

Here, we characterized the spatial organization of the *Nppa-Nppb* cluster in the normal and the stressed heart using 4C-seq (van de Werken et al., 2012). The regulatory potential of the contacting

Development (2016) 143, 2135-2146 doi:10.1242/dev.132019

sequences within the cluster were analyzed with chromatin immunoprecipitation (ChIP) for the enhancer-associated acetylated histone H3K27 (H3K27ac) and RNA polymerase II (Pol2). To identify regulatory elements involved in co-regulation of *Nppa* and *Nppb*, we made transgenic mice carrying modified bacterial artificial chromosomes (BACs) with reporter genes for both *Nppa* and *Nppb*, allowing the simultaneous monitoring of their dynamic expression patterns. Our study revealed that developmental and stress-induced expression of *Nppa* and *Nppb* is regulated by the interplay between shared developmental and non-shared stress-induced regulatory elements and dynamic epigenetic states within a 60-kb regulatory domain centered around *Nppb*.

RESULTS

The *Nppa-Nppb* cluster is organized in a permissive three-dimensional structure

To assess the topology of the *Nppa-Nppb* cluster and to define its potential regulatory domain, we characterized the interactions between different sequences (contact profiles) in the vicinity of *Nppa* and *Nppb* using high-resolution 4C-seq (Fig. 1A,B). Regulatory units are often flanked by CTCF-associated sites, where CCCTC-binding factor (CTCF) bound to DNA promotes DNA looping for proper regulation of gene expression (Lee and Iyer, 2012). The two closest CTCF-associated sites, located 41 kb upstream and 7 kb downstream of *Nppa*, were used as viewpoints. All regions contacting the viewpoints were sequenced and mapped to the genome. The median (±30% interval) of contact intensities (black curves and the gray bands, respectively, in Fig. 1B) show that the upstream CTCF-associated site (CTCF left) interacts with the downstream CTCF-associated site (CTCF right). Although vice versa interactions are less pronounced, these data indicate that the CTCF-associated sites encircle both *Nppa* and *Nppb* (Fig. 1A,B). The convergent orientation of these CTCF sites supports potential loop anchoring at the domain boundaries (Rao et al., 2014; de Wit et al., 2015). Moreover, both CTCF-associated sites interact with the *Nppa* promoter and another region within the locus (black arrowheads), showing possible involvement in the regulation of *Nppa* expression.

The data obtained from the promoter viewpoints indicate that interactions of both *Nppa* and *Nppb* are enriched between the CTCF-associated sites (Fig. 1B, second and third color-coded heatmaps from the top). *Nppb* lies in the center of these interactions with limited contacts beyond the CTCF sites. Although *Nppa* interactions are more widespread, most of them are concentrated within the 60-kb region flanked by the CTCF sites. Moreover, *Nppa* contacts are unidirectional and oriented towards *Nppb*. Interactions between the promoters of *Nppa* and *Nppb* are difficult to assess because the distance between these promoters is close to the spatial resolution of the 4C-seq analysis. *Nppa* and *Nppb* both interact with a region located 35 kb upstream of *Nppa* (black arrowheads). The interactions within the *Nppa-Nppb* locus are not heart specific, as they are also present in the liver (Fig. 1C; Fig. 2B), where *Nppa* and *Nppb* are not expressed. In both tissues, interactions of the CTCF-associated sites with the surrounding sequences are unipolar, contacting mostly the *Nppa-Nppb* locus (Fig. 1C, arrows). The frequency of these contacts is higher in the heart than in the liver. By contrast, interaction frequencies on the opposite side of the viewpoints are similar in both tissues (Fig. 1C, blue/red curves).

We next assessed whether the other genes in the vicinity in a 200-kb DNA region are co-expressed in the heart and respond to cardiac stress similarly to *Nppa* and *Nppb*, which would suggest co-regulation of these genes within the region. The expression levels of ten genes surrounding *Nppa* and *Nppb* were measured in adult ventricles by qPCR (Fig. 1D). Ventricular expression of *Nppa* decreases after birth (Horsthuis et al., 2008) to a level lower than that of *Nppb*. However, mRNA levels of *Nppa* were in large excess (7-170×) over that of the other genes in the locus. In the pressure-overloaded heart, 4 weeks after transverse aortic constriction (TAC) surgery, the heart weight (HW) to tibia length (TL) ratio and the levels of *Nppa* and *Nppb* were increased compared with control mice (Fig. 1E,F), whereas the expression of the other genes was not significantly changed (Fig. 1E). Therefore, among ten genes in this 200-kb DNA region, only *Nppa* and *Nppb* are highly expressed in the myocardium and induced after stress, suggesting that *Nppa* and *Nppb* do not share regulatory sequences with the surrounding genes. This analysis indicates that the sequences that regulate *Nppa* and *Nppb* lie within the 60-kb region flanked by CTCF-associated sites and form an *Nppa-Nppb* regulatory interaction domain. The conformation of this domain is not heart specific, although higher frequencies of interactions within the domain in the heart might contribute to the regulation of heart-specific *Nppa* and *Nppb* expression.

To locate discrete potential regulatory sequences in the 60-kb *Nppa-Nppb* regulatory domain in the fetal heart and during disease, we analyzed contacts of the *Nppa* and *Nppb* promoters with other sequences inside their interaction domain. We aligned cardiac ChIP-seq data for the CTCF sites with the 4C contact profiles generated from different heart regions and liver (Fig. 2A,B; Fig. S1). The bait regions in the promoters of *Nppa* and *Nppb* interact with each other as well as with the regions located between −35 kb and +7 kb relative to *Nppa* (red regions in the heatmaps). Notably, the patterns of these interactions are similar in the atria, fetal and adult ventricles, stressed ventricles, and even in the liver. Paired analysis of the adult and stressed ventricles, as well as the ventricles and the liver revealed that the interaction frequencies between the *Nppb* promoter and contact sites are similar (Fig. 2C). Taken together, the conformation of the *Nppa-Nppb* locus is permissive, i.e. not different between stages, tissues or conditions.

Localized stress-induced changes in H3K27ac and Pol2 association profiles within the *Nppa-Nppb* regulatory domain

We assessed the distribution and levels of H3K27ac, a chromatin modification associated with active enhancers, and the occupancy of Pol2, a mark of active promoters and enhancers. H3K27ac modification and Pol2 association are heart specific within the *Nppa-Nppb* interaction domain (gray area and magenta arrowheads) in a 200-kb DNA region (Fig. 3A). To assess whether the levels of H3K27ac and Pol2 occupancy are altered in the stressed heart, we performed ChIP-qPCR analysis in the ventricles of control and TAC mice 4 weeks after the operation. H3K27ac and Pol2 marks were enriched around *Nppa* and *Nppb* as well as in the region −40/−30 kb upstream of *Nppa* in control hearts (Fig. 3B,D). These data correspond to the ENCODE data for H3K27ac and Pol2 in the heart (Stamatoyannopoulos et al., 2012) (Fig. 3C). H3K27ac association was significantly different in the TAC hearts at many sites, whereas Pol2 occupancy changed much less. Increased H3K27ac was observed in the *Nppa* and *Nppb* promoters as well as at −18 kb, +2.3 kb and +15 kb relative to *Nppa*. Interestingly, the acetylation levels at the region 35-40 kb upstream of *Nppa* were decreased in TAC hearts compared with controls. Decreased Pol2 association at −37 kb relative to *Nppa* accompanied these changes.

Taken together, these data indicate global changes in H3K27ac association in the *Nppa-Nppb* regulatory domain after stress, with increased levels close to the genes, and decreased levels of both

Development (2016) 143, 2135-2146 doi:10.1242/dev.132019

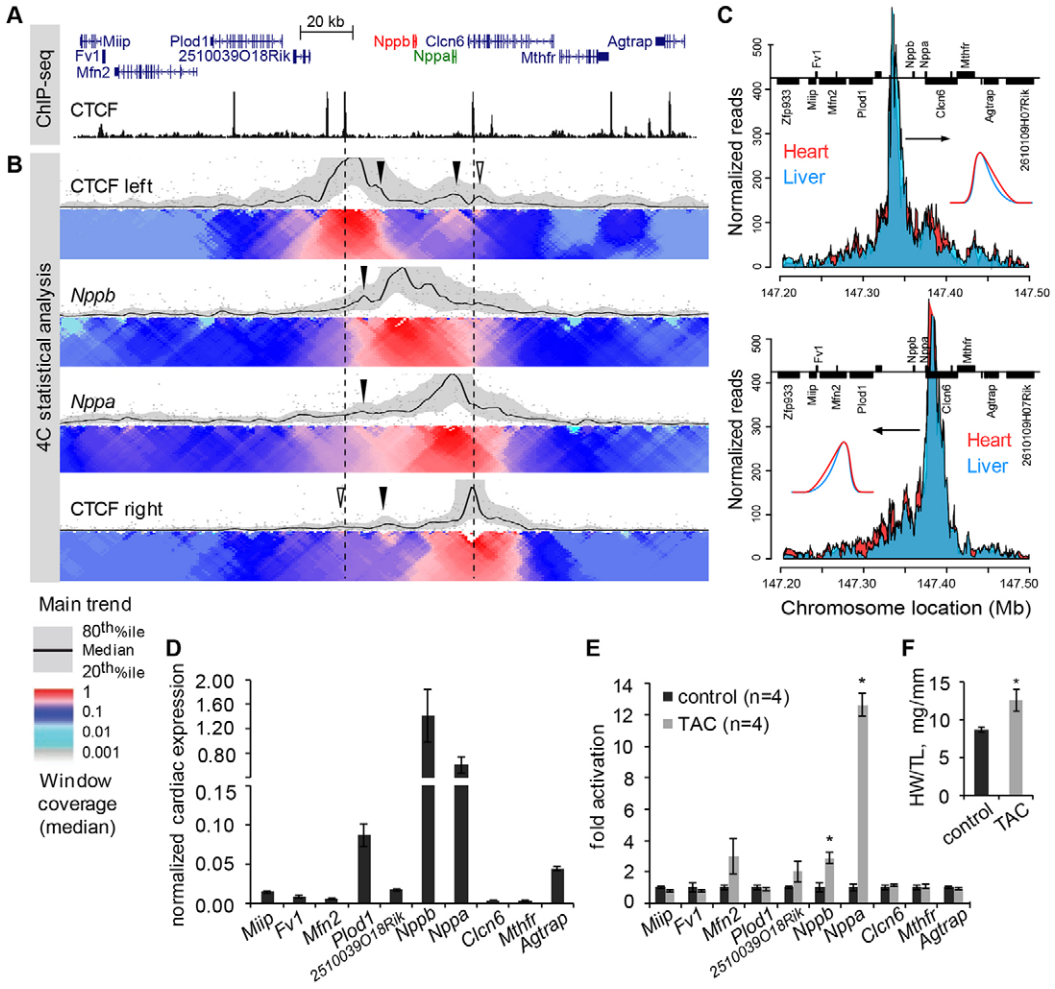

Fig. 1. Organization of the *Nppa-Nppb* locus. (A) UCSC genome browser view of ChIP-seq data of the CTCF-binding sites (Stamatoyannopoulos et al., 2012). (B) Integrated local contact profile analysis for *Nppb* and *Nppa*, and two CTCF-associated sites (dashed lines) used as viewpoints. Each top panel represents normalized contact intensities (gray dots), their running median (black line) analyzed with 4-kb sliding window, and the 20-80% percentile for these windows (gray band). In each bottom panel, the contact intensities, computed using linearly increasing sliding windows [scaled 2 (top) - 50 kb (bottom)], are displayed as a color-coded heatmap of positive 4C signals (maximum of interaction set to 1) (van de Werken et al., 2012). Local color changes are log-scaled to indicate changes of enrichment of captured sequences, corresponding to the DNA interaction. Black arrowheads indicate chromosome interaction between a viewpoint and potential regulatory regions, open arrowheads indicate interactions between the CTCF sites. (C) Comparison of the normalized reads in the heart and the liver samples for the left (top) and right (bottom) CTCF-associated sites as viewpoints. Arrows indicate more prevalent interactions of the viewpoints with the *Nppa-Nppb* locus, the blue/red curves represent a model of more prevalent interactions in the heart compared with the liver. (D) Ventricular expression of ten genes surrounding *Nppa* and *Nppb* was measured by qPCR (n=4). (E) Upregulation of mRNA levels of the locus genes in the ventricles 4 weeks after TAC surgery, analyzed by qPCR. Only *Nppa* and *Nppb* mRNA levels are significantly upregulated (P=4.3×10^{-6} and P=0.007, respectively; Student's two-tailed t-test). (F) Heart weight (HW) to tibia length (TL) ratio was significantly increased in the TAC-operated animals compared with the controls (P=0.045, Student's two-tailed t-test). Error bars represent s.e.m.

H3K27ac and Pol2 association in the conserved upstream region previously associated with developmental regulation of *Nppa* expression (Horsthuis et al., 2008).

Distal regulatory regions control the developmental expression of *Nppa* and *Nppb*

To test potential enhancer activity of parts of the region contacting the *Nppa* and *Nppb* promoters, individual fragments covering the region from −27 kb to +58 kb relative to *Nppa* were tested in transient transfection assays. Two fragments at −22 kb and at −11 kb relative to *Nppa* showed enhancer activity (not shown) and a moderate increase of H3K27ac levels at these regions after TAC (Fig. 3B). We generated transgenic mice with these fragments coupled to the *Nppa* basic promoter and EYFP reporter. Both −22-pr*Nppa*-EYFP and −11-pr*Nppa*-EYFP reporter constructs provided the expression pattern in the fetal heart typical of *Nppa* (Fig. 4A,D). Deletion of the −22 kb fragment from BAC336-KL did not impair the fetal expression pattern of *Luciferase* (reporting for *Nppa* activity) (Fig. 4G). These data suggest the presence of several redundant developmental *Nppa* enhancers.

To test the requirement of potential regulatory fragments in the context of the *Nppa-Nppb* locus, we generated a series of overlapping and truncated BAC double-reporter transgenic mice and compared the developmental profile and stress response of the reporter genes with those of the original BAC336 (Figs 5 and 6). The proximal promoter of *Nppa* present in all BACs contains sufficient information to drive robust atrial expression in embryonic and adult hearts (Horsthuis et al., 2008). Therefore, we report the expression levels of both *Luciferase/EGFP* (*Nppa* reporter) and *Katushka* (*Nppb* reporter) in fetal and adult ventricles relative to the

Development (2016) 143, 2135-2146 doi:10.1242/dev.132019

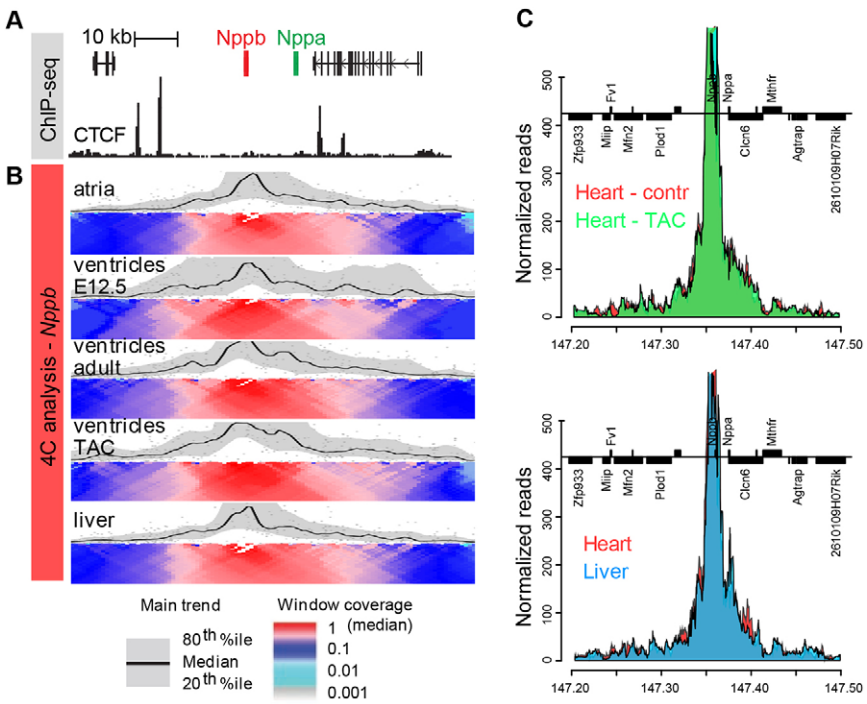

Fig. 2. Contact profiles of *Nppb* are similar during heart development and stress. (A) UCSC genome browser view of ChIP-seq data of the CTCF-binding sites (Stamatoyannopoulos et al., 2012). (B) Integrated contact profile for the *Nppb* viewpoint is similar between different tissues. Panel details are described in Fig. 1B. (C) Comparison of the normalized reads in the control versus TAC heart (top), and in the heart versus the liver (bottom) samples for the *Nppb* promoter as a viewpoint.

levels of atrial *Luciferase/EGFP* in each BAC mouse line. Two independent transgenic lines of BAC336-KL(I) and of BAC336-KL-Δdown(II) showed similar dynamic ventricular expression of *Luciferase* and *Katushka* (Fig. S2). Therefore, we further compared the expression of the reporters between different BAC transgenic lines.

The expression patterns of *Katushka* and *Luciferase* in BAC336-KL(I) recapitulated the expression pattern of *Nppb* and *Nppa*, respectively (Fig. 5A,B). Deletion of the downstream sequences in BAC336-KL-Δdown(II) or intergenic sequences in BAC336-KL-Δinter(III) did not alter the expression patterns of *Luciferase* and *Katushka* (Fig. 5B; data not shown). By contrast, deletion of the upstream sequences in BAC337-KE(IV) resulted in undetectable *Katushka* and reduced *EGFP* expression (Fig. 5B, lower panel). Quantification of the fetal ventricular activity of *Luciferase/EGFP* and *Katushka* by qPCR in the transgenic BAC lines confirmed these results (Fig. 5C,D). These findings suggest the presence of fetal ventricular enhancers of *Nppa* and *Nppb* in the distal upstream region (>27 kb upstream of *Nppa*).

Deletion of the downstream region in BAC336-KL-Δdown(II) and the intergenic region in BAC336-KL-Δinter(III) did not impair *Nppa*-characteristic postnatal downregulation of *Luciferase* (Fig. 5C). Similarly, the moderate decrease of *Nppb* after birth was recapitulated by the BAC transgenics lacking the downstream or intergenic region, although the postnatal decrease in reporter expression was stronger (Fig. 5D). Adult ventricular expression of *Katushka* was reduced in BAC337-KE(IV) and BAC336-KL-Δup(V) in which sequences more than 27 kb and 17 kb upstream of *Nppa*, respectively, were deleted. These data indicate that adult ventricular enhancers of *Nppb* are located upstream of the gene.

We next determined whether *Luciferase*/*EGFP* and *Katushka* are controlled by the same regulatory elements (Fig. 5E). Adult ventricular expression of *Luciferase*/*EGFP* and *Katushka* were significantly reduced in all the lines with the modified BACs (II-V) compared with those of *Luciferase* and *Katushka* in BAC336-KL(I), respectively. This analysis suggests either the presence of multiple regulatory regions upstream, in between and downstream of both genes, or an influence of the disturbed conformation of the locus resulting from the deletions. However, because of the multiple copies of the BACs integrated in the genome, interpretation of the 4C-seq data from these BAC lines was not possible (data not shown). The levels of *Katushka* in BAC336-KL-Δdown(II), BAC336-KL-Δinter(III) and BAC336-KL-Δup(V) were consistently higher than those of *Luciferase*, mimicking the ratio of endogenous *Nppa/Nppb* (Fig. 5E). However, in BAC337-KE(IV), which lacks the upstream region, the ratio between *EGFP* and *Katushka* expression levels in the ventricles was reversed and significantly different from that in BAC336-KL(I) (Fig. 5E, insert). These data indicate that the distal upstream region is required for adult basal ventricular activity of *Nppb*. In BAC336-KL-Δup(V), ventricular *Luciferase* levels were again lower than *Katushka* levels, suggesting that adult ventricular *Nppa* expression is regulated by sequences located from −27 to −17 kb relative to *Nppa*.

Taken together, we conclude that prenatal ventricular expression of *Nppa* and *Nppb* are co-regulated by, possibly shared, distal upstream elements, but that postnatal expression involves different elements. Our data also suggest that the topology of the locus, influenced by the deletions, affects the regulation of the *Nppa-Nppb* cluster.

Stress-response elements are different from the developmental regulatory elements

To test whether the two developmental enhancers located −22 and −11 kb upstream of *Nppa* contain stress-response elements, the −22-pr*Nppa*-EYFP and −11-pr*Nppa*-EYFP reporter mice were subjected to TAC surgery. EYFP expression levels were not induced in the ventricles 4 weeks after TAC surgery (Fig. 4B,C,E,F). Moreover, the levels of *Nppa* correlated with that of *Luciferase* in the ventricles of BAC336-KL-Δ(−22) mice after TAC (Fig. 4H,I). Therefore, the −22 kb and −11 kb regions, which contribute to the developmental expression of *Nppa*, are not involved in its stress-induced upregulation. Similarly, the levels of *Katushka* mRNA increased after TAC and mimicked that of *Nppb*, showing that the −22 kb fragment is not involved in stress-induced upregulation of *Nppb* (Fig. 1H).

Development (2016) 143, 2135-2146 doi:10.1242/dev.132019

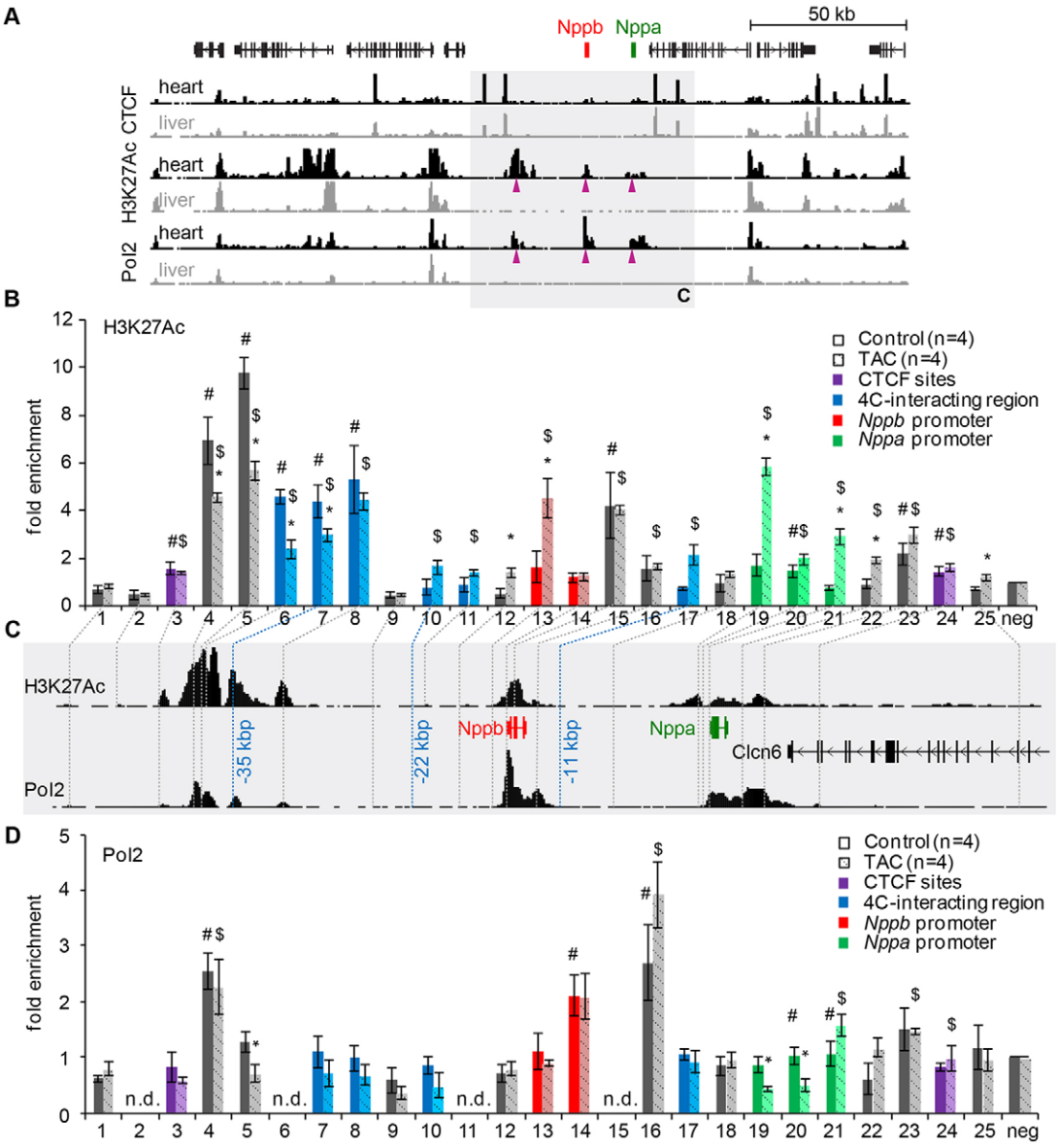

Fig. 3. Epigenetic features of the *Nppa-Nppb* locus. (A) UCSC genome browser view of the ChIP-seq data of the CTCF- and Pol2-binding sites, and H3K27ac marks in the heart and liver (Stamatoyannopoulos et al., 2012). Magenta arrowheads indicate heart-specific modifications within the domain surrounded by the CTCF-associated sites (gray area). (B,D) Changes of H3K27ac (B) and Pol2 binding (D) measured by ChIP-qPCR in the ventricles 4 weeks after TAC surgery. *$P \leq 0.05$ versus control (Student's *t*-test); $^{\#}P \leq 0.05$ versus negative region in control; $^{\$}P \leq 0.05$ versus negative region in TAC (Wilcoxon one-sample test). Error bars represent s.e.m. (C) UCSC genome browser view of ChIP-seq data of H3K27ac and Pol2 (Stamatoyannopoulos et al., 2012) within the region depicted in gray in A. Vertical lines indicate the positions of the primers for ChIP-qPCR.

To identify stress-response region(s) of *Nppb* and *Nppa*, we analyzed the induction of reporter gene expression in the other BAC transgenic mice after TAC. The induction of *Katushka* and *Luciferase* mRNA in BAC336-KL(I) mice after TAC recapitulates the induction of *Nppb* and *Nppa*, respectively (Sergeeva et al., 2014). We compared the response of the reporters in the reference BAC336-KL(I) line with that in other transgenic lines that lack regions contacting the *Nppa/Nppb* promoters (Fig. 6, Figs S3, S4 and Table S1). This comparison allowed us to assess the necessity of critical regulatory regions for *Nppa* and/or *Nppb* induction.

Deletion of the region downstream of *Nppa* in BAC336-KL-Δdown(II) and of the 12-kb intergenic region in BAC336-KL-Δinter(III) did not reduce the TAC-induced response of *Katushka* and *Luciferase* in the ventricles compared with BAC336-KL(I) (Fig. 6). Although the response of *Luciferase* in one of two independent lines of BAC336-KL-Δdown(II) is significantly stronger than that in BAC336-KL(I), we interpret both lines as containing sufficient regulatory information for reporter induction (Fig. S5). These data reveal that the potential enhancers are located in the regions upstream of *Nppb*, in agreement with the loss of the stress response of *Luciferase* in RP23-139J21(VI) (Fig. 6, Fig. S3). Deletion of the sequences upstream of −27 kb in BAC337-KE(IV) and of −17.2 kb in BAC336-KL-Δup(V) relative to *Nppa*, resulted in reduced reporter gene activity in the adult ventricles (Fig. 5E). Nevertheless, EGFP expression (*Nppa* reporter) in BAC337-KE(IV) was upregulated after TAC, whereas analogous expression of *Luciferase* in BAC336-KL-Δup(V) was not (Fig. 6, Fig. S3). By contrast, the response of *Katushka* (*Nppb* reporter) to stress was decreased in both lines compared with that in BAC336-KL(I),

Development (2016) 143, 2135-2146 doi:10.1242/dev.132019

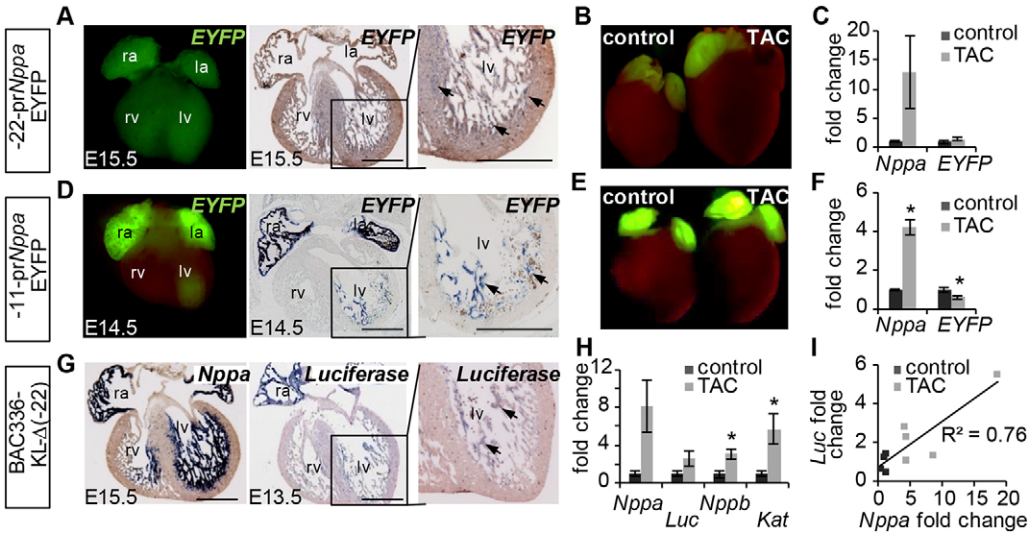

Fig. 4. Two regions contacting *Nppa* regulate its developmental, but not stress-induced expression. (A,D) Potential regulatory elements located −22 kb and −11 kb relative to *Nppa* were coupled to the *Nppa* promoter and EYFP reporter, which recapitulated expression of *Nppa* in the atria and trabecular fetal ventricular myocardium. (B,E) EYFP fluorescence in −22-pr*Nppa*-EYFP and −11-pr*Nppa*-EYFP mice mimicked atrial expression of *Nppa* in the adult hearts, but did not increase in the left ventricular myocardium of the TAC hearts compared with the controls. Two representative hearts are shown. (C,F) *Nppa* mRNA levels analyzed by qPCR increased in the ventricles 4 weeks after TAC surgery whereas *EYFP* mRNA levels was not changed in −22-pr*Nppa*-EYFP mice (C) (n=4 control and n=3 TAC; P=0.225 for *Nppa* and P=0.06 for *EYFP*) or decreased in −11-pr*Nppa*-EYFP mice (F) (n=3 control and n=3 TAC; P=0.028 for *Nppa* and P=0.0002 for *EYFP*). (G) Deletion of the −22 region Δ(−22) from BAC336-KL did not impair ventricular transmural pattern of *Luciferase* in E15.5 transgenic mice. (H) *Nppa*, *Luciferase*, *Nppb* and *Katushka* mRNA levels analyzed by qPCR were upregulated in the ventricles of BAC336-KL-Δ(−22) mice 2 weeks after TAC (n=4 control and n=5 TAC; P=0.064 for *Nppa*, P=0.117 for *Luciferase*, P=0.013 for *Nppb*, P=0.043 for *Katushka*). (I) Correlation of *Nppa* and *Luciferase* levels in the ventricular myocardium of the control and operated BAC336-KL-Δ(−22) mice (P=0.002). Student's two-tailed t-test was used in C,F,H; t-test between the slopes of the regression lines was used in I. Error bars indicate s.e.m. la, left atrium; lv, left ventricle; ra, right atrium; rv, right ventricle. Arrows in A,D,G indicate EYFP expression in trabeculated myocardium. Scale bars: 0.5 mm; 0.2 mm (zoomed panels).

although these differences did not reach statistical significance (Fig. 6; Figs S3 and S4; lines IV and V). Therefore, sequences located >27 kb upstream of *Nppa* might contribute to stress-induced *Nppb* expression. However, sequences crucial for *Nppa* upregulation are located in the region between −27 and −22 kb upstream of *Nppa*, implying that different mechanisms regulate *Nppa* and *Nppb*.

Because the promoters of *Nppa* and *Nppb* were shown to interact with each other (Fig. 1B), we deleted the 0.6-kb *Nppb* promoter in BAC336-KL(I) to assess its contribution to stress-induced *Nppa* expression. The response of *Luciferase* to stress in BAC336-KL-Δpr*Nppb*(VII) mice was completely abrogated compared with that in BAC336-KL(I) (Fig. 6; Fig. S3). These data suggest that the *Nppb* proximal promoter is required for *Nppa* upregulation during stress. A 2-kb *Nppb* promoter fragment exhibits enhancer activity when tested in neonatal rat ventricular myocytes (NRVM) stimulated with phenylephrine (Fig. S6). However, this 2-kb *Nppb* promoter fragment coupled to the 0.7-kb *Nppa* promoter-*Luciferase* was not sufficient to induce *Luciferase* expression in the stressed heart (Fig. 6; Fig. S3). These data indicate that the *Nppb* promoter contains regulatory information contributing to, but not sufficient for stress-induced expression of *Nppa in vivo*.

Taken together, we conclude that *Nppa* stress-response enhancers are different from its developmental regulatory sequences. Induction of *Nppa* after stress is dependent on the *Nppb* promoter and the sequences located in the region from −27 to −22 kb relative to *Nppa*. *Nppb* basal ventricular activity, as well as stress-induced expression, is regulated by the sequences located >27 kb upstream of *Nppa*. Therefore, stress-induced reactivation of *Nppa* and *Nppb* is regulated by different mechanisms.

3D conformation model of the *Nppa-Nppb* cluster during development and disease

The 4C-seq analysis of the chromosome conformation of the *Nppa-Nppb* locus revealed interactions occurring between several potential regulatory regions (Fig. 2) within a 60-kb domain flanked by CTCF-associated sites. Inside this domain, −41/−30 kb, −15/−11 kb (containing *Nppb*) and −0.7/+4 kb (containing *Nppa*) regions relative to *Nppa* contain regulatory elements as predicted by the EMERGE enhancer prediction tool (van Duijvenboden et al., 2016) (Fig. 7A). This prediction correlates well with the developmental and stress-induced enhancer regions identified in our functional studies using transgenic mice (Fig. 7A). Taking the dynamic ventricular expression of *Nppa* and *Nppb* into account (Fig. 7B), we constructed a functional 3D model of the *Nppa-Nppb* locus (Fig. 7C). In this model, a chromatin loop anchored by the convergent CTCF sites encloses *Nppa*, *Nppb* and their regulatory regions. Although the promoters of *Nppa* and *Nppb* interact with each other and with the sequences located up to 40 kb upstream of *Nppa*, different sets of regions are involved in the dynamic regulation of expression of these two genes. The region >27 kb upstream of *Nppa*, presumably the −41/−30 kb element, regulates embryonic, adult and stress-induced expression of *Nppb*. Supposedly, dynamic levels of H3K27ac association with this region as well as with the promoter of *Nppb* might contribute to the relatively modest changes of *Nppb* expression in the postnatal and stressed heart. By contrast, *Nppa* ventricular expression dramatically decreases after birth and increases after stress (Fig. 7B). Therefore, the *Nppa* promoter is modulated by several regulatory elements, some of which are shared with *Nppb*. Postnatal downregulation of *Nppa* might be governed by the sequences located −27 to −22 kb relative to its start, but during stress *Nppa*

Development (2016) 143, 2135-2146 doi:10.1242/dev.132019

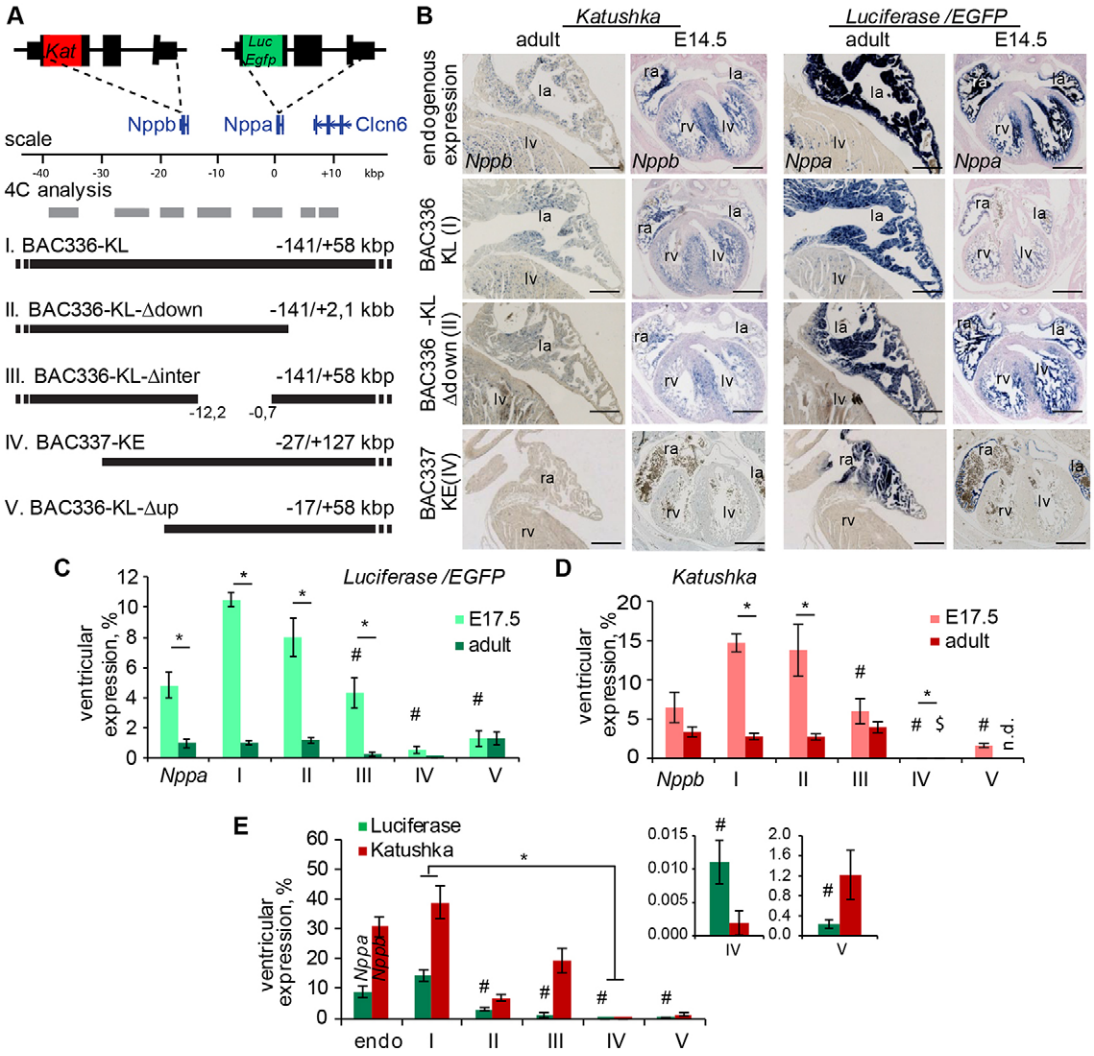

Fig. 5. Developmental enhancers of *Nppa* and *Nppb* are located upstream of both genes. (A) Overview of the overlapping BACs and BAC deletion clones (black lines) with a schematic of interacting regions (gray lines) as identified by 4C-seq. BAC reporter constructs were modified with *Katushka* and *Luciferase*/*EGFP* (KL/E) genes inserted at the *Nppb* and *Nppa* translation start sites, respectively. (B) Expression pattern of *Nppb* and *Nppa* (top panels), and the corresponding *Katushka* and *Luciferase*/*EGFP* (lower panels) in the fetal and adult hearts of the transgenic mouse lines was studied with *in situ* hybridization. Only in the absence of the upstream region (BAC337-KEIV), was *Katushka* expression undetectable. (C-E) Fetal and adult ventricular *Luciferase*/*EGFP* and *Katushka* expression levels in different BAC lines, measured by qPCR, were corrected to the levels of fetal atrial *Luciferase*/*EGFP* of each line (n=3-6). In the absence of the upstream region in BAC337-KE(IV) and BAC336-KL-Δup(V), postnatal downregulation of *EGFP*/*Luciferase* is abolished because of low fetal ventricular activity of the reporter (C), and both fetal and adult *Katushka* ventricular activity are reduced compared with that in BAC336-KL(I). (D) Expression levels of *Katushka* in the adult heart of BAC336-KL-Δup(V) were close to the detection limit and, therefore, the adult ventricular activity was not determined. *P<0.05 E17.5 versus adult, $^{\#,\$}P$<0.05 versus line I. (E) Comparison of adult ventricular *Katushka* and *Luciferase*/*EGFP* activity in different transgenic lines shows dysregulation of the reporter expression in BAC337-KE(IV) and BAC336-KL-Δup(V). $^{\#}P$<0.05 versus line I, *P<0.05 *Luciferase(EGFP)*/*Katushka* ratio versus line I. Student's two-tailed t-test was used in C-E; error bars represent s.e.m. Scale bars: 0.5 mm.

additionally functionally interacts with the *Nppb* promoter, which is required, but not sufficient, for *Nppa* upregulation. The proposed model indicates that the regulatory information of the gene cluster is distributed across the locus rather than present specifically in one or a few shared discrete enhancers, and predicts that the 3D conformation and changes in epigenetic state of the locus contribute to the regulation of *Nppa* and *Nppb* during development and disease.

DISCUSSION

The *Nppa-Nppb* cluster is confined to a regulatory domain

The expression levels of *Nppa* and *Nppb* are almost exclusively heart specific (Gardner et al., 1987) and were by far the highest of the ten genes in the 200-kb DNA region around the cluster. The selective cardiac-specific expression and coordinated induction of *Nppa* and *Nppb* during hypertrophy suggest the presence of regulatory elements in the locus selectively targeting these genes.

Promoters and their regulatory elements interact with each other within topologically associated domains (TADs). TADs are separated by boundary regions enriched for convergent CTCF-associated sites (Ong and Corces, 2014; Rao et al., 2014; de Wit et al., 2015). Our 4C-seq analysis indicates that the CTCF-associated sites flanking *Nppa/Nppb* contact each other, encircling the gene promoters and most of their interaction partners. Although we have not shown the requirement of the CTCF sites for *Nppa/Nppb* regulation, we suggest that CTCF protein complexes anchor the loop using the convergent CTCF-binding sequences and maintain the stability of the regulatory

Development (2016) 143, 2135-2146 doi:10.1242/dev.132019

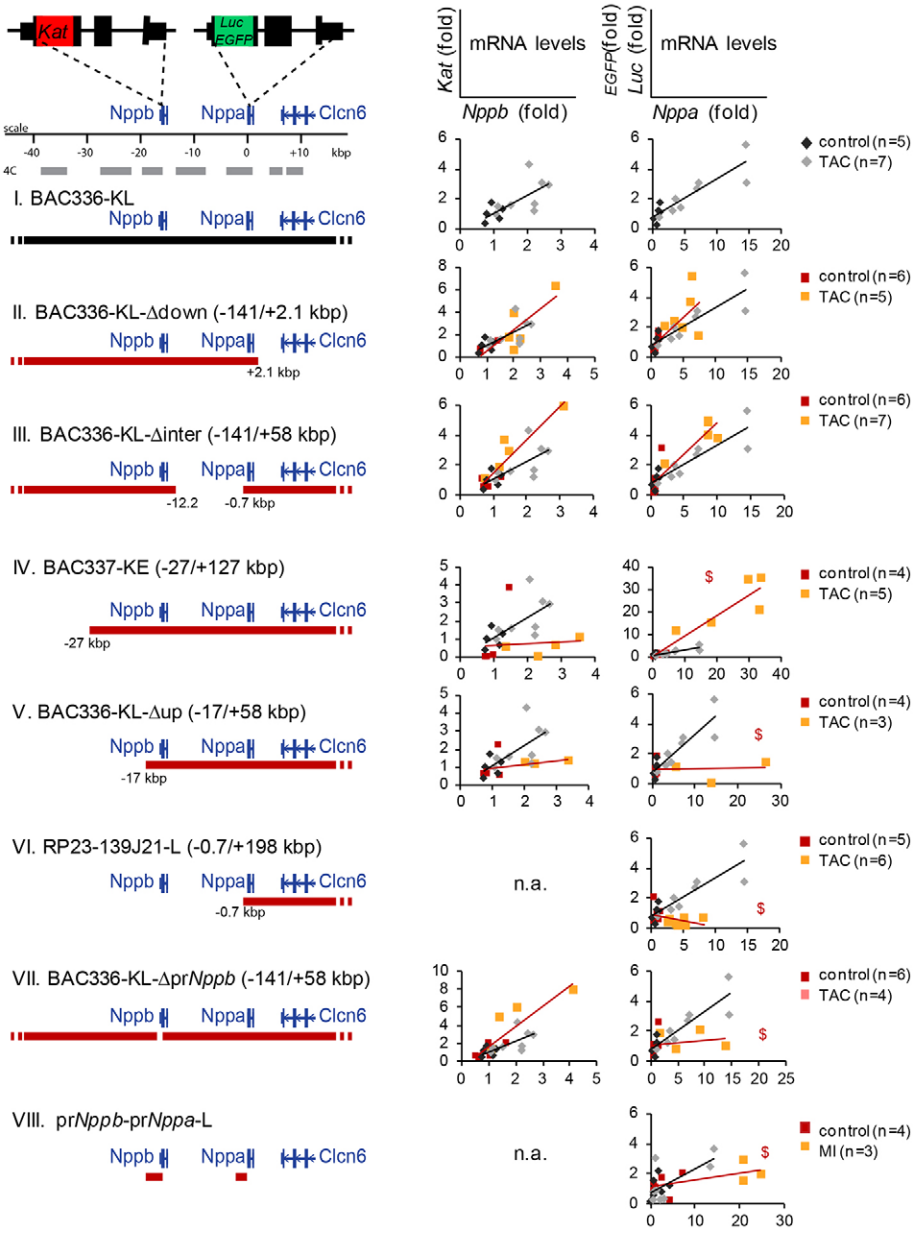

Fig. 6. Overview of the activity of regulatory *Nppa* and *Nppb* sequences during stress. BAC336-KL (black line), overlapping BACs and BAC deletion clones (red lines) with inserted *Katushka* and *Luciferase*/*EGFP* reporters, and a schematic of interacting regions (gray lines) as identified by 4C-seq are presented in the left panel. Correlation between *Nppb* and *Katushka* mRNA levels, and between *Nppa* and *Luciferase*/*EGFP* mRNA levels in the ventricular myocardium of the control and operated transgenic mice are shown in the scatterplots in the right panel. Correlation of each pair of genes in the transgenic lines II-VIII (represented in red/orange) was compared with those in BAC336-KL(I) (represented in black/gray), which contains all necessary information for the stress response. mRNA levels of the genes were measured by qPCR 2 weeks (I) or 2-4 weeks (II-VII) after TAC surgery, or 1 week after MI (VIII). $^{\$}P<0.05$ versus BAC336-KL(I) (*t*-test between the slopes of the regression lines).

domain. Moreover, the upstream CTCF site might also be associated with enhancer elements, because this region contacts the *Nppa* promoter and is enriched for H3K27ac, H3K4me1, p300 and DNaseI hypersensitive sites (HSs), indicative of potential enhancer activity. Furthermore, the topology of the locus was similar in atria, ventricles and liver, and in fetal and adult stages, qualifying the conformation of the *Nppa-Nppb* locus as permissive, where the contacts are pre-formed and not cell type dependent (de Laat and Duboule, 2013).

TAD boundaries are static across species and cell types (Dekker et al., 2013). When comparing the organization of the *Nppa/Nppb*-containing region in the mouse heart with that in other tissues we found that the 60-kb regulatory domain is a structural subunit of a larger ~600-kb TAD. The upstream border of this TAD in mouse cerebellar cortex and embryonic stem cells coincides with the boundary we observed with 4C-seq and is relatively sharp (Dixon et al., 2012). Downstream of *Nppa*, interactions gradually decrease by the position of *Clcn6* (20 kb downstream *Nppa*), as observed by 4C-seq, suggesting a much less strict boundary between the 60-kb domain and the remainder of the TAD. This (sub)domain organization suggests the establishment of a rigid chromatin organization already at very early stages in mouse development. Hi-C data from several human cell lines, performed with higher resolution compared with the mouse 4C-seq data, indicates the presence of a 100-kb domain similar to the mouse 60-kb domain, i.e. including only *NPPA*, *NPPB* and a conserved region upstream of both genes (Rao et al., 2014).

Previously, genome-wide association studies have identified genetic variants influencing the concentration of natriuretic peptides in the blood of heart failure patients. Two single nucleotide polymorphisms, rs5065 in an exon of *NPPA* (Vassalle et al., 2007) and rs1023252 in an intron of *CLCN6* (Del Greco et al., 2011), showed association with NT-proBNP (N-terminal of the prohormone brain natriuretic peptide) levels in patients with cardiac dysfunction, indicating that these variants can affect the function of regulatory sequences. Genetic variants associated with hypertension (Flister et al., 2013) are positioned across a larger 300-kb region (from upstream of *NPPB* to downstream of

Development (2016) 143, 2135-2146 doi:10.1242/dev.132019

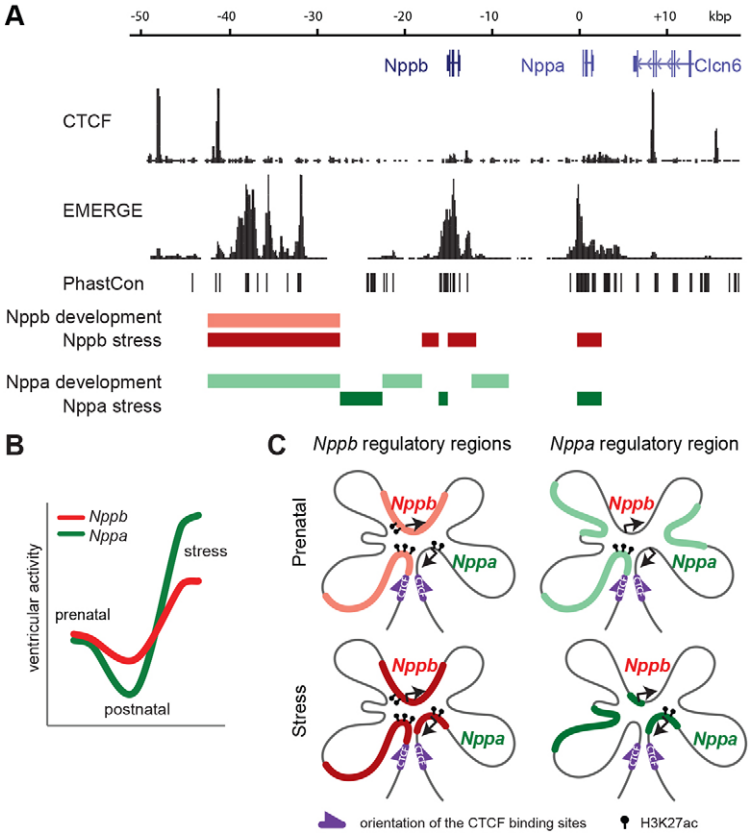

Fig. 7. Three-dimensional functional model of the *Nppa-Nppb* locus. (A) Developmental and stress-response regions of *Nppa* and *Nppb* are located within the 60-kb region confined between CTCF-associated sites (Stamatoyannopoulos et al., 2012) and overlapping with the predicted enhancers (van Duijvenboden et al., 2016). Red bars, developmental and stress-response regions of *Nppb*; green bars, developmental and stress-response regions of *Nppa*. (B) Ventricular downregulation of *Nppa* in the ventricles after birth and upregulation during stress is more remarkable than the same changes of *Nppb* expression. (C) *Nppa* and *Nppb* are regulated by different mechanisms during development and stress. *Nppb* expression relies on the interaction of the promoter with a single upstream enhancer region, where the levels of H3K27ac may contribute to *Nppb* regulation. The *Nppa* promoter cooperates with several different regulatory elements to regulate its dynamic expression in the embryonic and adult heart.

AGTRAP). Because blood pressure is influenced by multiple genes within this region (*MTHFR*, *CLCN6*, *NPPA*, *NPPB*), these data suggest that the variants influence the expression of several genes within the TAD, including *NPPA* and *NPPB*. As these variants are in linkage disequilibrium, it is not yet known which variants influence the expression of *NPPA* and *NPPB*. Our data suggest that variants that influence *NPPA/NPPB* expression, and thus predispose to hypertension, are localized within the 60-kb regulatory domain.

Clustered *Nppa* and *Nppb* share developmental but not stress-response enhancers

Three natriuretic peptide genes developed during vertebrate evolution by duplication of a common ancestral gene. Mammals retain *Nppa* and *Nppb*, conserved among species and positioned at a distance of only 15 kb from each other in the genome (Inoue et al., 2003). Several studies of clustered genes describe coordinated regulation by shared regulatory sequences (Nolte et al., 2013; Tena et al., 2011). Given the highly similar spatiotemporal expression patterns of *Nppa* and *Nppb*, we hypothesized that these clustered genes might also share regulatory elements.

Previously, the region from −27 to +58 kb relative to *Nppa* was found to contain regulatory elements required for the stress-response of *Nppa*, whereas upstream sequences are responsible for its developmental activity (Horsthuis et al., 2008; Sergeeva and Christoffels, 2013). Three potential enhancer elements at −35, −31 and −21 kb relative to *Nppa* were identified based on their ability to bind Nkx2-5 *in vivo*. These elements, when combined, were able to drive correct prenatal ventricular expression, but they could not activate the *lacZ* reporter in the ventricles after TAC (Warren et al., 2011). A 650-bp conserved element at −37 kb upstream of *Nppa* was able to induce Luciferase expression in the ventricles of transgenic mice after TAC (Matsuoka et al., 2014). However, this element is located outside the region required for stress responsiveness of *Nppa*. These data suggest the presence of multiple enhancers regulating *Nppa*, and possibly *Nppb*, during disease. Our analysis of BAC transgenic mice revealed that *Nppa* and *Nppb* share some developmental enhancers located >27 kb upstream of *Nppa*. The highly conserved 10-kb DNA region located at −40/−30 kb of *Nppa* contains many DNaseI HS sites, sites occupied by cardiac transcription factors, p300, and histone modifications associated with gene regulation. This region contacts the promoters of both *Nppa* and *Nppb* and might represent a fetal ventricular enhancer region of these genes. Furthermore, this region might be involved in the basal and stress-induced expression of *Nppb* in the adult heart. Therefore, we suggest that the 650-bp fragment (Matsuoka et al., 2014) located within the −40/−30 kb region is one of the distal stress-response enhancers of *Nppb*, not *Nppa*. In support of this notion, we observed very strong *EGFP* (reporting for *Nppa*) upregulation in the stressed ventricles of BAC337-KE(IV) mice lacking the entire −40/−30 kb region.

We observed that the mouse *Nppb* promoter was required for basal *Nppb* expression in the fetal and adult heart, but not required

Development (2016) 143, 2135-2146 doi:10.1242/dev.132019

for its stress induction. Furthermore, the *Nppb* promoter induced *Luciferase* expression in neonatal rat ventricular myocytes stimulated with phenylephrine, and was necessary, but not sufficient, for *Nppa* stress induction *in vivo*. Two previous studies found that the 408-bp human and 534-bp rat *Nppb* promoters were able to stimulate expression to some extent in myocardial infarction (MI) or angiotensin II-induced hypertrophy, respectively (He et al., 2001; Majalahti et al., 2007). Together, these data suggest that the promoter of *Nppb* might be part of a composite stress-inducing enhancer for *Nppa*, acting as a scaffold attracting other regulatory DNA elements and transcription factors for combinatorial enhancer activity in the context of the proper chromatin conformation and histone modifications. Because the randomly integrated BACs are not suitable for *in vivo* 4C-seq analysis, this hypothesis has to be tested by deletion of the region from the mouse genome using genome-editing technologies.

Although BACs usually provide an accurate expression pattern of the integrated transgene, they have some weaknesses related to the random site of integration, copy number and integrity. Therefore, we confirmed proper reporter gene expression in two independent founder lines for some of the BACs, and analyzed several overlapping BACs to confirm the results of individual transgenic lines. Taking the activities of the reporter genes in all mouse lines into account, we conclude that potential *Nppa* stress-response elements are located in the region from −27 to −22 kb relative to *Nppa*. Although ChIP-seq data sets indicate that this region does not bind cardiac transcription factors, part of this region interacts with the promoter of *Nppa*. Together, these data show that the clustered *Nppa* and *Nppb* genes share their developmental enhancers, but not their stress-response elements. Because fetal expression and stress-induced *Nppa* induction appear to be dependent on different enhancers, fetal expression and reactivation of the 'fetal gene program' during stress require different transcriptional mechanisms.

Histone modifications in the *Nppa-Nppb* cluster during hypertrophy

Histone modifications, such as acetylation or methylation of lysine residues of histone H3, are involved in transcriptional regulation. Such modifications have been associated with the development of cardiomyopathies in the adult heart (Mahmoud and Poizat, 2013). Demethylation of H3K9 at the promoter regions of *NPPA* and *NPPB* was associated with activation of their expression in failing human left ventricular myocardium, whereas H3K9ac was not changed and H3K27ac was modestly increased (Hohl et al., 2013), in accordance with our observations (Fig. 3B, red and green bars). Both *Nppa* and *Nppb* have been reported to recruit Pol2 *de novo* 4 days after TAC (Sayed et al., 2013). We did not observe significant changes in Pol2 binding at the promoter regions of *Nppa* and *Nppb* 4 weeks after TAC, presumably because phosphorylation of Pol2 at the transcription start site of *Nppa* is required for activation of its expression (Spiltoir et al., 2013). Although it is likely that the promoter regions participate in the induction of both genes, the mouse *Nppa* (Horsthuis et al., 2008; Knowlton et al., 1995) and *Nppb* (this study) promoters were not sufficient to provide the stress response. Therefore, distal elements must be required for the induction of *Nppa* and *Nppb*.

Genome-wide analysis of H3K27ac revealed that many loci are differentially associated with acetylated H3K27 during hypertrophy in mice (Papait et al., 2013). Close analysis of these data showed that H3K27ac levels were slightly increased at the promoter regions of *Nppa* and *Nppb*, but were not markedly changed in the −22 kb and −11 kb putative regulatory regions, in line with our findings. However, the −40/−35 kb region relative to *Nppa*, described above as a potential enhancer, was highly acetylated already in the normal heart (our data; Papait et al., 2013; Stamatoyannopoulos et al., 2012), and is likely to be involved in the adult expression of *Nppb*, which, in contrast to *Nppa*, is still expressed in the ventricles after birth. After TAC, the levels of H3K27ac in this region were significantly lower than in the normal heart. These variations in acetylation at specific loci might be involved in modulation of transcription factor binding (Reynolds et al., 2013) at enhancers for fine-tuning of *Nppa/Nppb* expression. Taken together, the data point to global epigenetic changes in the locus, which, in conjunction with multiple enhancers and in the context of a three-dimensional conformation convey the stress response to the transcriptional activity of *Nppa* and *Nppb*.

MATERIALS AND METHODS

Animals

Animal care and experiments conform to the Directive 2010/63/EU of the European Parliament. All animal work was approved by the Animal Experimental Committee of the Academic Medical Center, Amsterdam, and was carried out in compliance with the Dutch government guidelines. Transgenic mice (*Mus musculus*) were generated and bred on the FVB/N background. See supplementary Materials and Methods for further details.

4C-seq experiments

Preparation of 4C templates was described previously (Simonis et al., 2009). In short, adult mouse hearts and liver were isolated, dissociated and homogenized to obtain a single cell suspension. Chromatin was cross-linked with 2% formaldehyde, nuclei were isolated, and cross-linked DNA was digested with *Dpn*II. Digestion was followed by proximity ligation, removal of cross-links, a secondary restriction digestion with *Csp*6I and a second proximity ligation. For all experiments, 200 ng of the resulting 4C template was used for the subsequent PCR reaction. After PCR, 4C templates were purified, bar-coded, mixed and sequenced simultaneously on Illumina HiSeq 2000 platform. Mapping and filtering of the sequence reads was carried out as previously described (van de Werken et al., 2012). See supplementary Materials and Methods for further details, including primer design, data analysis and statistics.

Chromatin immunoprecipitation

Left ventricles of the control and TAC hearts were dissected, ground in liquid nitrogen and cross-linked in 1% formaldehyde. Cross-linking was quenched, tissues were further dissociated and lysed. Cross-linked nuclei were sonicated under conditions established to yield an average fragment size of ∼300 bp. Antibodies were anti-H3K27ac (2 µg; Abcam, ab4729) and anti-Pol II (2 µg; Santa Cruz Biotech, sc-899X). Immunoprecipitation, washing, elution, and reverse cross-linking were performed as previously described (van den Boogaard et al., 2013). ChIP-qPCR was performed on a Roche LightCycler 480 System using Sybr Green monitoring. The ratio of ChIPed DNA normalized for input DNA was compared with that of a negative control region within *Hprt* and is presented as fold enrichment. See supplementary Materials and Methods for further details, including primer sequences.

BAC and vector constructs

Generation of BAC336-Katushka-Luciferase [BAC336-KL(I)] and BAC337-EGFP has been described previously (Horsthuis et al., 2008; Sergeeva et al., 2014). See supplementary Materials and Methods for further details of all constructs.

Transverse aortic constriction

Wild-type or transgenic FVB/N male mice (8-12 weeks old) were subjected to transverse aortic constriction (TAC) as described (van Deel et al., 2011). All mice were weighed, sedated with 4% isoflurane and anesthetized with O_2/N_2 (v/v=1/2) containing 2.5% isoflurane. Buprenorphine (50 µg/kg) was injected subcutaneously for postsurgical analgesia. Age-matched unbanded

Development (2016) 143, 2135-2146 doi:10.1242/dev.132019

littermates were used as controls. After 4 weeks, the ventricular apex was used for qPCR and the left ventricle was fixed for 4C and ChIP experiments. Ventricular tissue was dissected and apportioned for qPCR and *in situ* hybridization. See supplementary Materials and Methods for further details.

Myocardial infarction

Infarction was created in 8- to 12-week-old BAC336KL and pr*Nppb*-pr*Nppa*-Luc male mice by permanent ligation of the left anterior descending coronary artery according to the protocol described previously (De Celle et al., 2004) with slight modifications. Mice were sedated with 4% isoflurane, analgesized subcutaneously with buprenorphine (0.068 mg/kg) and intubated. Anesthesia was maintained with 2% isoflurane in O_2 (1 l/min flow rate). After 1 week, the border zone of the operated mice and a piece of left ventricle of the control mice were dissected and used for qPCR analysis. See supplementary Materials and Methods for further details.

RNA isolation and RT-qPCR

Dissected atrial and ventricular tissue of embryonic, control adult and TAC/MI-operated mice was dissected and snap frozen in liquid nitrogen and stored at −80°C. Total RNA was isolated using Trizol Reagent according to the manufacturer's protocol (Invitrogen). Three-hundred nanograms (fetal tissue) or 500 ng (adult tissue) of total RNA was used for reverse transcription with the Superscript II system (Invitrogen) and Oligo-dT as primers. Expression of different genes was assayed by quantitative real-time PCR using the LightCycler Real-Time PCR system (Roche Diagnostics). Values were normalized to *Gapdh* and *Hprt* expression levels. See supplementary Materials and Methods for further details, including primer sequences.

In situ hybridization

Non-radioactive *in situ* hybridization on sections was performed as described previously (Moorman et al., 2001). Embryos and hearts were fixed in 4% formaldehyde, embedded in paraplast and sectioned at 10 µm. The cDNA probes used were *Nppa*, *Nppb*, *Luciferase*, *Katushka* and *EYFP*. Images were acquired with the Zeiss Axiophot microscope. See supplementary Materials and Methods for further details.

Lentiviral enhancer assay

Lentivirus development

Three fragments were PCR amplified from the mouse BAC336 clone containing the *Nppa* and *Nppb* loci (129 SvJ BAC library, Incyte, St Louis, MO, USA). The PCR fragments were subcloned into the lentiviral vector encoding the firefly luciferase reporter (pGreenFire Transcriptional Reporter Lentivector; System Biosciences, Mountain View, CA, USA). The supernatant from 293T cells containing the lentiviral particles was collected 48 and 72 h after transfection and concentrated by centrifugation in Amicon Ultra-15 Centrifugal Filter Unit (Millipore, UFC910008).

Cardiac myocytes, fibroblasts and luciferase assay

Rat neonatal ventricular myocytes (NRVMs) and fibroblasts were isolated from 1- to 2-day-old Lewis rats, infected with the lentiviral vectors and incubated for 16 h. Subsequently, the cells were exposed to 100 µM phenylephrine (Sigma, P6126-10G) for 48 h. Cell extracts and luciferase assay were performed according to the manufacturer's protocol using the *Renilla* Luciferase Assay System (Promega) and the Glomax-Multi detection system. See supplementary Materials and Methods for further details.

Statistical analysis of *in vivo* experiments

Fetal and adult ventricular *Luciferase/EGFP* and *Katushka* expression levels were normalized to the levels of fetal atrial *Luciferase/EGFP* (Fig. 2C,D). All data in bar charts are represented as mean value±s.e.m. The two-tailed Student's *t*-test was used to determine statistical significance ($P<0.05$) of the differences between the fetal [embryonic day (E) 17.5] and adult ventricular activity of the reporter genes, and the differences in normalized ventricular activity between different BAC transgenic lines and those of BAC336KL(I). In TAC and MI experiments, factor correction (Ruijter et al., 2006) was used to remove variability between experiments performed in several sessions. The two-tailed Student's *t*-test was used to determine statistical significance ($P<0.05$) of gene upregulation. Correlation coefficients were used to determine the relationship between the levels of *Nppb* and *Katushka* mRNA, and the levels of *Nppa* and *Luciferase/EGFP* mRNA, which represent the response of the reporter genes to stress. A *t*-test between the slopes of the regression lines was used to estimate the difference between the response of the reporter genes in two transgenic lines (Armitage et al., 2008). See supplementary Materials and Methods for further details.

Acknowledgements

We acknowledge the assistance and support of the Animal Research Institute of the Academic Medical Center (AMC), University of Amsterdam, in generating the BAC transgenic mouse lines. We thank Vincent Wakker for help in generating transgenic constructs and Corrie de Gier-de Vries for *in situ* hybridization.

Competing interests

The authors declare no competing or financial interests.

Author contributions

I.A.S. performed experiments and analyzed data; I.B.H., I.v.d.M. and N.E.d.G. provided technical assistance, E.E.C. supervised I.v.d.M. and N.E.d.G.; J.M.R. performed statistical analysis; H.J.G.v.d.W. performed 4C analysis; I.A.S. and V.M.C. wrote the manuscript; V.M.C. and E.E.C. obtained funding; V.M.C. supervised the research team.

Funding

This work was supported by the TRIUMPH project [01C-103] within the Center for Translational Molecular Medicine; the Netherlands Cardiovascular Research Initiative (CVON) HUSTCARE project; and Fondation Leducq. E.E.C. was supported by grants from the Netherlands Organization for Scientific Research (Nederlandse Organisatie voor Wetenschappelijk Onderzoek) [NWO-836.12.002 and 825.13.007] and the Netherlands Cardiovascular Research Initiative [CVON-ARENA-2011-11].

Data availability

The GEO accession number for the 4C data reported in this paper is GSE81057.

Supplementary information

Supplementary information available online at
http://dev.biologists.org/lookup/suppl/doi:10.1242/dev.132019/-/DC1

References

Bruneau, B. G. (2011). Atrial natriuretic factor in the developing heart: a signpost for cardiac morphogenesis. *Can. J. Physiol. Pharmacol.* **89**, 533-537.

Cameron, V. A., Aitken, G. D., Ellmers, L. J., Kennedy, M. A. and Espiner, E. A. (1996). The sites of gene expression of atrial, brain, and C-type natriuretic peptides in mouse fetal development: temporal changes in embryos and placenta. *Endocrinology* **137**, 817-824.

De Celle, T., Cleutjens, J. P., Blankesteijn, W. M., Debets, J. J., Smits, J. F. and Janssen, B. J. (2004). Long-term structural and functional consequences of cardiac ischaemia-reperfusion injury in vivo in mice. *Exp. Physiol.* **89**, 605-615.

de Laat, W. and Duboule, D. (2013). Topology of mammalian developmental enhancers and their regulatory landscapes. *Nature* **502**, 499-506.

de Wit, E., Vos, E. S. M., Holwerda, S. J. B., Valdes-Quezada, C., Verstegen, M. J. A. M., Teunissen, H., Splinter, E., Wijchers, P. J., Krijger, P. H. L. and de Laat, W. (2015). CTCF binding polarity determines chromatin looping. *Mol. Cell* **60**, 676-684.

Dekker, J., Marti-Renom, M. A. and Mirny, L. A. (2013). Exploring the three-dimensional organization of genomes: interpreting chromatin interaction data. *Nat. Rev. Genet.* **14**, 390-403.

Del Greco, M. F., Pattaro, C., Luchner, A., Pichler, I., Winkler, T., Hicks, A. A., Fuchsberger, C., Franke, A., Melville, S. A., Peters, A. et al. (2011). Genome-wide association analysis and fine mapping of NT-proBNP level provide novel insight into the role of the MTHFR-CLCN6-NPPA-NPPB gene cluster. *Hum. Mol. Genet.* **20**, 1660-1671.

Dixon, J. R., Selvaraj, S., Yue, F., Kim, A., Li, Y., Shen, Y., Hu, M., Liu, J. S. and Ren, B. (2012). Topological domains in mammalian genomes identified by analysis of chromatin interactions. *Nature* **485**, 376-380.

Flister, M. J., Tsaih, S.-W., O'Meara, C. C., Endres, B., Hoffman, M. J., Geurts, A. M., Dwinell, M. R., Lazar, J., Jacob, H. J. and Moreno, C. (2013). Identifying multiple causative genes at a single GWAS locus. *Genome Res.* **23**, 1996-2002.

Gardner, D. G., Vlasuk, G. P., Baxter, J. D., Fiddes, J. C. and Lewicki, J. A. (1987). Identification of atrial natriuretic factor gene transcripts in the central nervous system of the rat. *Proc. Natl. Acad. Sci. USA* **84**, 2175-2179.

Guo, J., Gan, X. T., Haist, J. V., Rajapurohitam, V., Zeidan, A., Faruq, N. S. and Karmazyn, M. (2011). Ginseng inhibits cardiomyocyte hypertrophy and heart failure via NHE-1 inhibition and attenuation of calcineurin activation. *Circ. Heart Fail.* **4**, 79-88.

He, Q., Wang, D., Yang, X. P., Carretero, O. A. and LaPointe, M. C. (2001). Inducible regulation of human brain natriuretic peptide promoter in transgenic mice. *Am. J. Physiol. Heart Circ. Physiol.* **280**, 368-376.

Hohl, M., Wagner, M., Reil, J.-C., Müller, S.-A., Tauchnitz, M., Zimmer, A. M., Lehmann, L. H., Thiel, G., Böhm, M., Backs, J. et al. (2013). HDAC4 controls histone methylation in response to elevated cardiac load. *J. Clin. Invest.* **123**, 1359-1370.

Horsthuis, T., Houweling, A. C., Habets, P. E. M. H., de Lange, F. J., el Azzouzi, H., Clout, D. E., Moorman, A. F. and Christoffels, V. M. (2008). Distinct regulation of developmental and heart disease-induced atrial natriuretic factor expression by two separate distal sequences. *Circ. Res.* **102**, 849-859.

Houweling, A. C., Somi, S., Massink, M. P. G., Groenen, M. A., Moorman, A. F. M. and Christoffels, V. M. (2005). Comparative analysis of the natriuretic peptide precursor gene cluster in vertebrates reveals loss of ANF and retention of CNP-3 in chicken. *Dev. Dyn.* **233**, 1076-1082.

Inoue, K., Naruse, K., Yamagami, S., Mitani, H., Suzuki, N. and Takei, Y. (2003). Four functionally distinct C-type natriuretic peptides found in fish reveal evolutionary history of the natriuretic peptide system. *Proc. Natl. Acad. Sci. USA* **100**, 10079-10084.

Kathiriya, I. S., Nora, E. P. and Bruneau, B. G. (2015). Investigating the transcriptional control of cardiovascular development. *Circ. Res.* **116**, 700-714.

Knowlton, K., Rockman, H., Itani, M., Vovan, A., Seidman, C. and Chien, K. (1995). Divergent pathways mediate the induction of ANF transgenes in neonatal and hypertrophic ventricular myocardium. *J. Clin. Invest.* **96**, 1311-1318.

Lee, B.-K. and Iyer, V. R. (2012). Genome-wide studies of CCCTC-binding factor (CTCF) and cohesin provide insight into chromatin structure and regulation. *J. Biol. Chem.* **287**, 30906-30913.

Mahmoud, S. A. and Poizat, C. (2013). Epigenetics and chromatin remodeling in adult cardiomyopathy. *J. Pathol.* **231**, 147-157.

Majalahti, T., Suo-Palosaari, M., Sármán, B., Hautala, N., Pikkarainen, S., Tokola, H., Vuolteenaho, O., Wang, J., Paradis, P., Nemer, M. et al. (2007). Cardiac BNP gene activation by angiotensin II in vivo. *Mol. Cell. Endocrinol.* **273**, 59-67.

Matsuoka, K., Asano, Y., Higo, S., Tsukamoto, O., Yan, Y., Yamazaki, S., Matsuzaki, T., Kioka, H., Kato, H., Uno, Y. et al. (2014). Noninvasive and quantitative live imaging reveals a potential stress-responsive enhancer in the failing heart. *FASEB J.* **28**, 1870-1879.

Moorman, A. F. M. and Christoffels, V. M. (2003). Cardiac chamber formation: development, genes, and evolution. *Physiol. Rev.* **83**, 1223-1267.

Moorman, A. F. M., Houweling, A. C., de Boer, P. A. J. and Christoffels, V. M. (2001). Sensitive nonradioactive detection of mRNA in tissue sections: novel application of the whole-mount in situ hybridization protocol. *J. Histochem. Cytochem.* **49**, 1-8.

Nolte, C., Jinks, T., Wang, X., Martinez Pastor, M. T. and Krumlauf, R. (2013). Shadow enhancers flanking the HoxB cluster direct dynamic Hox expression in early heart and endoderm development. *Dev. Biol.* **383**, 158-173.

Ong, C.-T. and Corces, V. G. (2014). CTCF: an architectural protein bridging genome topology and function. *Nat. Rev. Genet.* **15**, 234-246.

Papait, R., Cattaneo, P., Kunderfranco, P., Greco, C., Carullo, P., Guffanti, A., Viganò, V., Stirparo, G. G., Latronico, M. V. G., Hasenfuss, G. et al. (2013). Genome-wide analysis of histone marks identifying an epigenetic signature of promoters and enhancers underlying cardiac hypertrophy. *Proc. Natl. Acad. Sci. USA* **110**, 20164-20169.

Rao, S. S. P., Huntley, M. H., Durand, N. C., Stamenova, E. K., Bochkov, I. D., Robinson, J. T., Sanborn, A. L., Machol, I., Omer, A. D., Lander, E. S. et al. (2014). A 3D map of the human genome at kilobase resolution reveals principles of chromatin looping. *Cell* **159**, 1665-1680.

Reynolds, N., O'Shaughnessy, A. and Hendrich, B. (2013). Transcriptional repressors: multifaceted regulators of gene expression. *Development* **140**, 505-512.

Sanyal, A., Lajoie, B. R., Jain, G. and Dekker, J. (2012). The long-range interaction landscape of gene promoters. *Nature* **489**, 109-113.

Sayed, D., He, M., Yang, Z., Lin, L. and Abdellatif, M. (2013). Transcriptional regulation patterns revealed by high resolution chromatin immunoprecipitation during cardiac hypertrophy. *J. Biol. Chem.* **288**, 2546-2558.

Sergeeva, I. A. and Christoffels, V. M. (2013). Regulation of expression of atrial and brain natriuretic peptide, biomarkers for heart development and disease. *Biochim. Biophys. Acta* **1832**, 2403-2413.

Sergeeva, I. A., Hooijkaas, I. B., Van Der Made, I., Jong, W. M. C., Creemers, E. E. and Christoffels, V. M. (2014). A transgenic mouse model for the simultaneous monitoring of ANF and BNP gene activity during heart development and disease. *Cardiovasc. Res.* **101**, 78-86.

Simonis, M., Klous, P., Homminga, I., Galjaard, R.-J., Rijkers, E.-J., Grosveld, F., Meijerink, J. P. P. and de Laat, W. (2009). High-resolution identification of balanced and complex chromosomal rearrangements by 4C technology. *Nat. Methods* **6**, 837-842.

Spiltoir, J. I., Stratton, M. S., Cavasin, M. A., Demos-Davies, K., Reid, B. G., Qi, J., Bradner, J. E. and McKinsey, T. A. (2013). BET acetyl-lysine binding proteins control pathological cardiac hypertrophy. *J. Mol. Cell. Cardiol.* **63**, 175-179.

Stamatoyannopoulos, J. A., Snyder, M., Hardison, R., Ren, B., Gingeras, T., Gilbert, D. M., Groudine, M., Bender, M., Kaul, R., Canfield, T. et al. (2012). An encyclopedia of mouse DNA elements (Mouse ENCODE). *Genome Biol.* **13**, 418.

Tena, J. J., Alonso, M. E., de la Calle-Mustienes, E., Splinter, E., de Laat, W., Manzanares, M. and Gómez-Skarmeta, J. L. (2011). An evolutionarily conserved three-dimensional structure in the vertebrate Irx clusters facilitates enhancer sharing and coregulation. *Nat. Commun.* **2**, 310.

Troughton, R., Michael Felker, G. and Januzzi, J. L. (2014). Natriuretic peptide-guided heart failure management. *Eur. Heart J.* **35**, 16-24.

van de Werken, H. J. G., Landan, G., Holwerda, S. J. B., Hoichman, M., Klous, P., Chachik, R., Splinter, E., Valdes-Quezada, C., Oz, Y., Bouwman, B. A. et al. (2012). Robust 4C-seq data analysis to screen for regulatory DNA interactions. *Nat. Methods* **9**, 969-972.

van Deel, E. D., de Boer, M., Kuster, D. W., Boontje, N. M., Holemans, P., Sipido, K. R., van der Velden, J. and Duncker, D. J. (2011). Exercise training does not improve cardiac function in compensated or decompensated left ventricular hypertrophy induced by aortic stenosis. *J. Mol. Cell. Cardiol.* **50**, 1017-1025.

van den Boogaard, M., Wong, L. Y. E., Christoffels, V. M. and Barnett, P. (2013). Acquisition of high quality DNA for massive parallel sequencing by in vivo chromatin immunoprecipitation. *Methods Mol. Biol.* **977**, 53-64.

van Duijvenboden, K., de Boer, B. A., Capon, N., Ruijter, J. M. and Christoffels, V. M. (2016). EMERGE: a flexible modelling framework to predict genomic regulatory elements from genomic signatures. *Nucleic Acids Res.* **44**, e42.

Vassalle, C., Andreassi, M. G., Prontera, C., Fontana, M., Zyw, L., Passino, C. and Emdin, M. (2007). Influence of ScaI and natriuretic peptide (NP) clearance receptor polymorphisms of the NP System on NP concentration in chronic heart failure. *Clin. Chem.* **53**, 1886-1890.

Warren, S. A., Terada, R., Briggs, L. E., Cole-Jeffrey, C. T., Chien, W.-M., Seki, T., Weinberg, E. O., Yang, T. P., Chin, M. T., Bungert, J. et al. (2011). Differential role of Nkx2-5 in activation of the atrial natriuretic factor gene in the developing versus failing heart. *Mol. Cell. Biol.* **31**, 4633-4645.

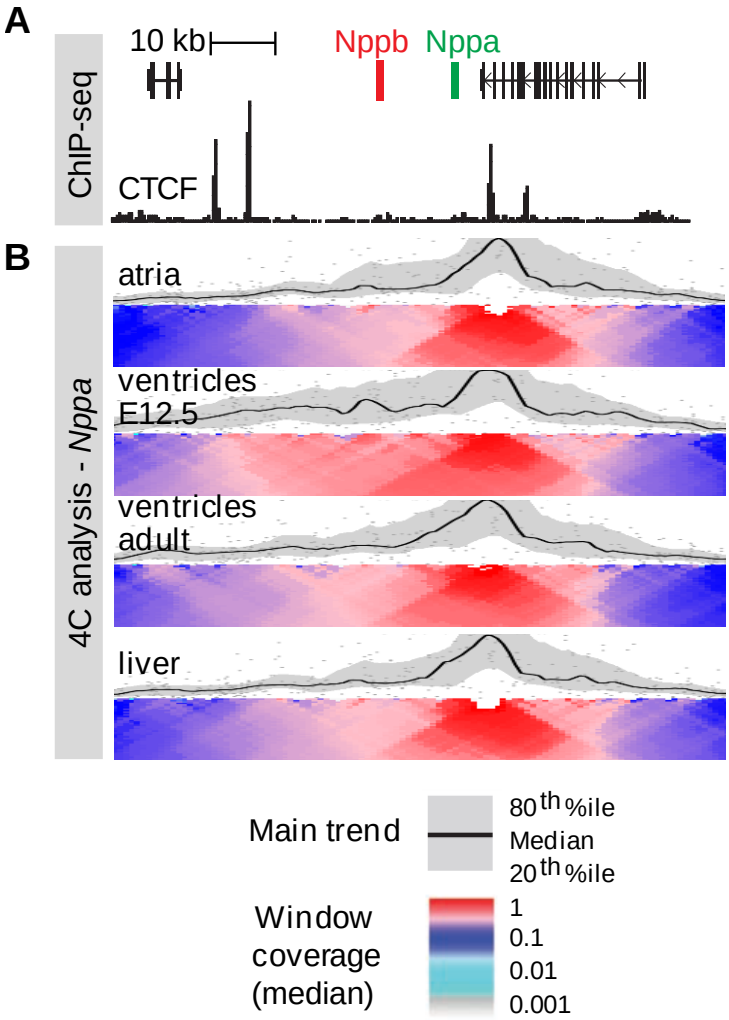

Fig. S1. Contact profiles of *Nppa* are similar during heart development and stress. (A) UCSC genome browser view of ChIP-seq data of the CTCF binding sites (Stamatoyannopoulos et al., 2012). (B) Integrated contact profile for the *Nppa* viewpoint is similar between different tissues. The top panel represents normalized contact intensities (gray dots), their running median (black line) analyzed with 4 kb sliding window, and the 20-80% percentile for these windows (gray band). In the bottom panel, contact intensities are computed using linearly increasing sliding windows (scaled 2 (top) - 50 kb (bottom)) and are displayed as a color-coded heatmap of positive 4C signals (maximum of interaction set to 1) (Werken et al., 2012b). Local color changes are log-scaled to indicate changes of statistical enrichment of captured sequences, corresponding to the DNA interaction.

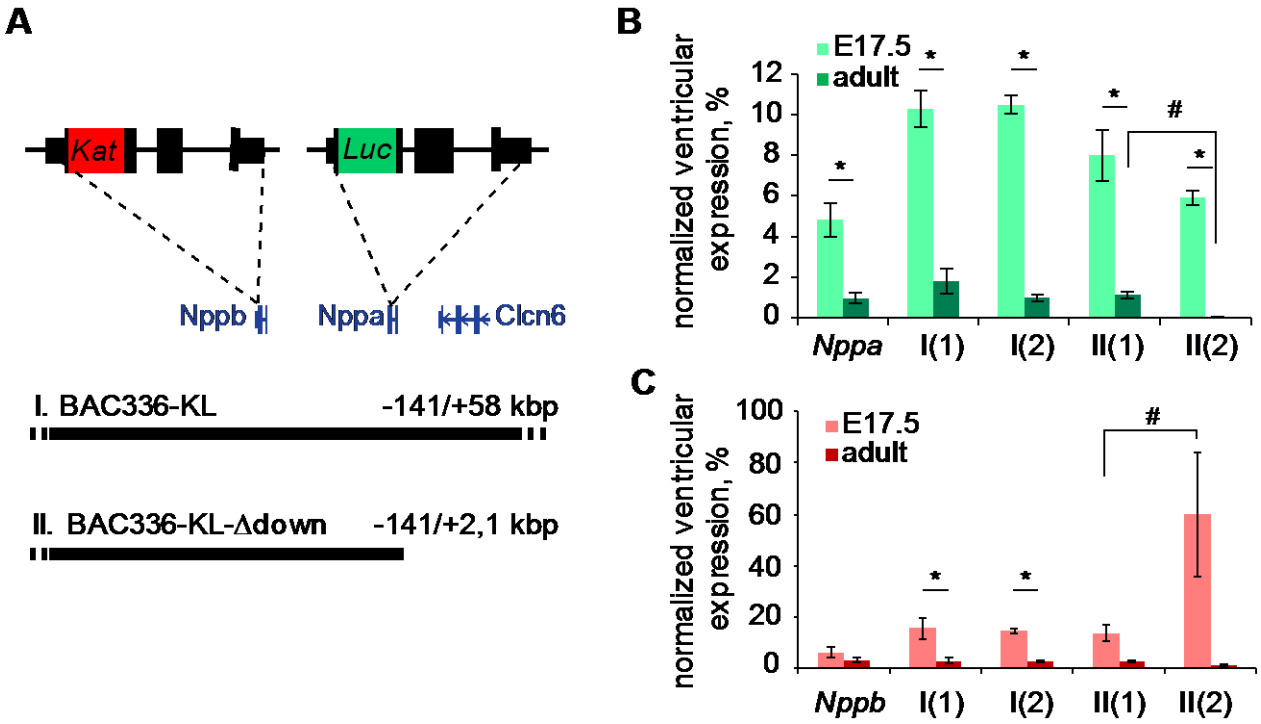

Fig. S2. Two independent founder lines exhibit similar developmental behavior of the reporter genes. (A) Schematic representation of BAC336-KL(I) and BAC336-KL-Δdown(II) constructs. BAC reporter constructs were modified with Katushka and Luciferase (KL) genes inserted into *Nppb* and *Nppa* translation start sites, respectively. (B,C) Normalized fetal and adult ventricular activity of *Luciferase* (B) and *Katushka* (C) measured with qPCR (n=3-6). *Luciferase* and *Katushka* were downregulated in the ventricles after birth, following significant and moderate downregulation of *Nppa* and *Nppb,* respectively. Although adult ventricular activities of *Luciferase* was lower and the fetal ventricular activity of *Katushka* was higher in line 2 of BAC336-KL-Δdown(II), the developmental behavior of the reporter genes remained comparable. The efficiency of BAC transgenesis after oocyte injection is usually lower than that of small plasmid-based constructs (Van Keuren et al., 2009). In this study, only one or two lines per BAC construct have been analyzed. However, some of the BAC constructs are complementary to each other in their coverage of the *Nppa-Nppb* locus (Figure 3, BAC336-KL-Δdown(II) and RP23-139J21-L(VI)). The data obtained from these mice validate each other's results, thus compensating for the lack of multiple independent lines per BAC. Student's two-tailed t-test was used in (B,C); *p<0.05 E17.5 vs. adult, $^{\#}$p<0.05 line (1) vs line (2). Error bars represent s.e.m.

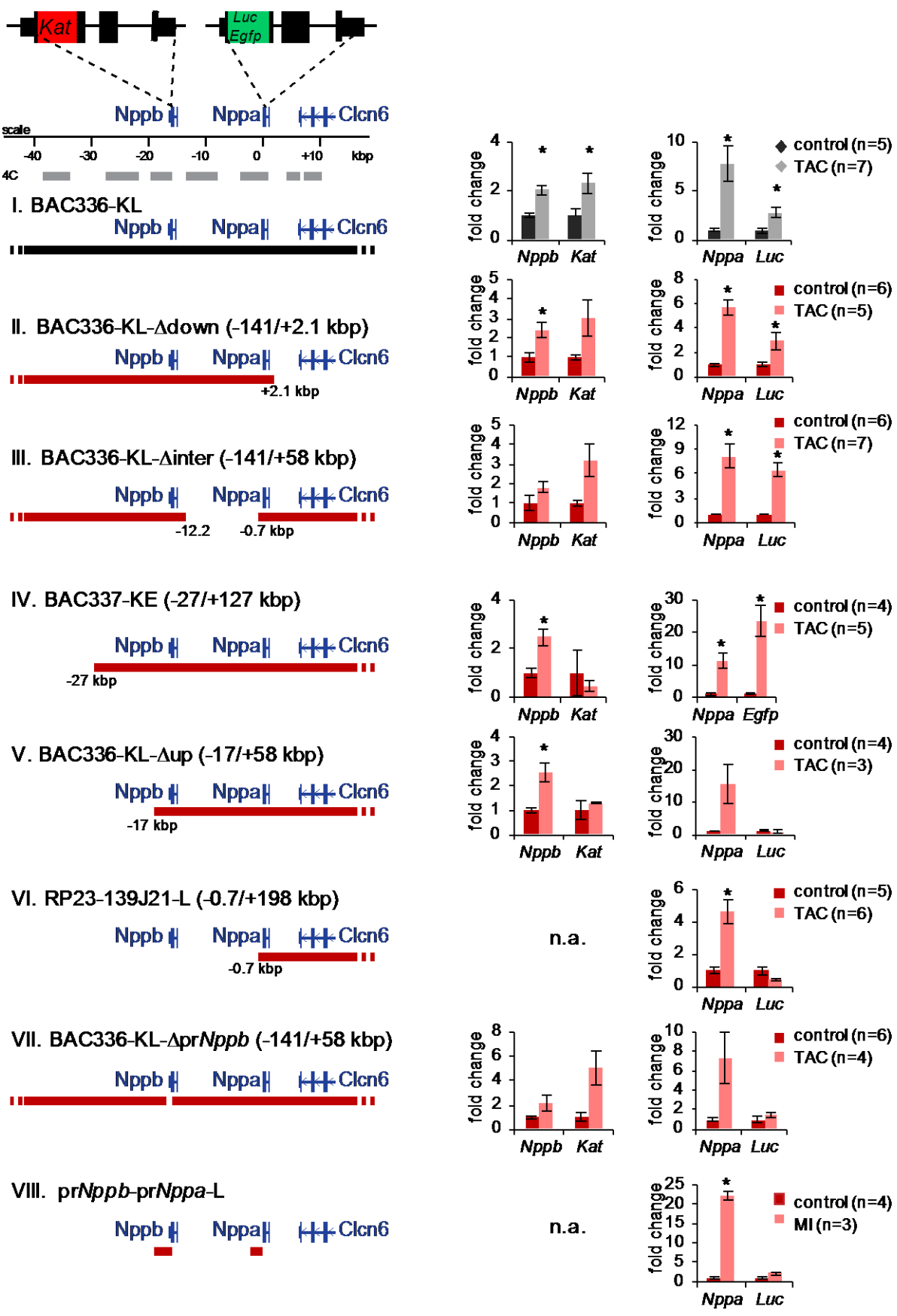

Fig. S3. Overview of the activity of regulatory *Nppa* and *Nppb* sequences during stress. BAC336-KL (black line), overlapping BACs and BAC deletion clones (red lines) with inserted *Katushka* and *Luciferase/EGFP*

reporters, and the schematic representation of interacting regions (gray lines) as identified by 4C-seq are presented in the left panel. Changes in mRNA levels of *Nppb, Katushka, Nppa* and *Luciferase/EGFP* are shown in the right panel. mRNA levels of the genes were measured with qPCR 2 weeks (I), 2-4 weeks (II-VII) after TAC surgery or 1 week after MI (VIII). *p<0.05 vs. control (Student's two-tailed t-test). Error bars represent s.e.m.

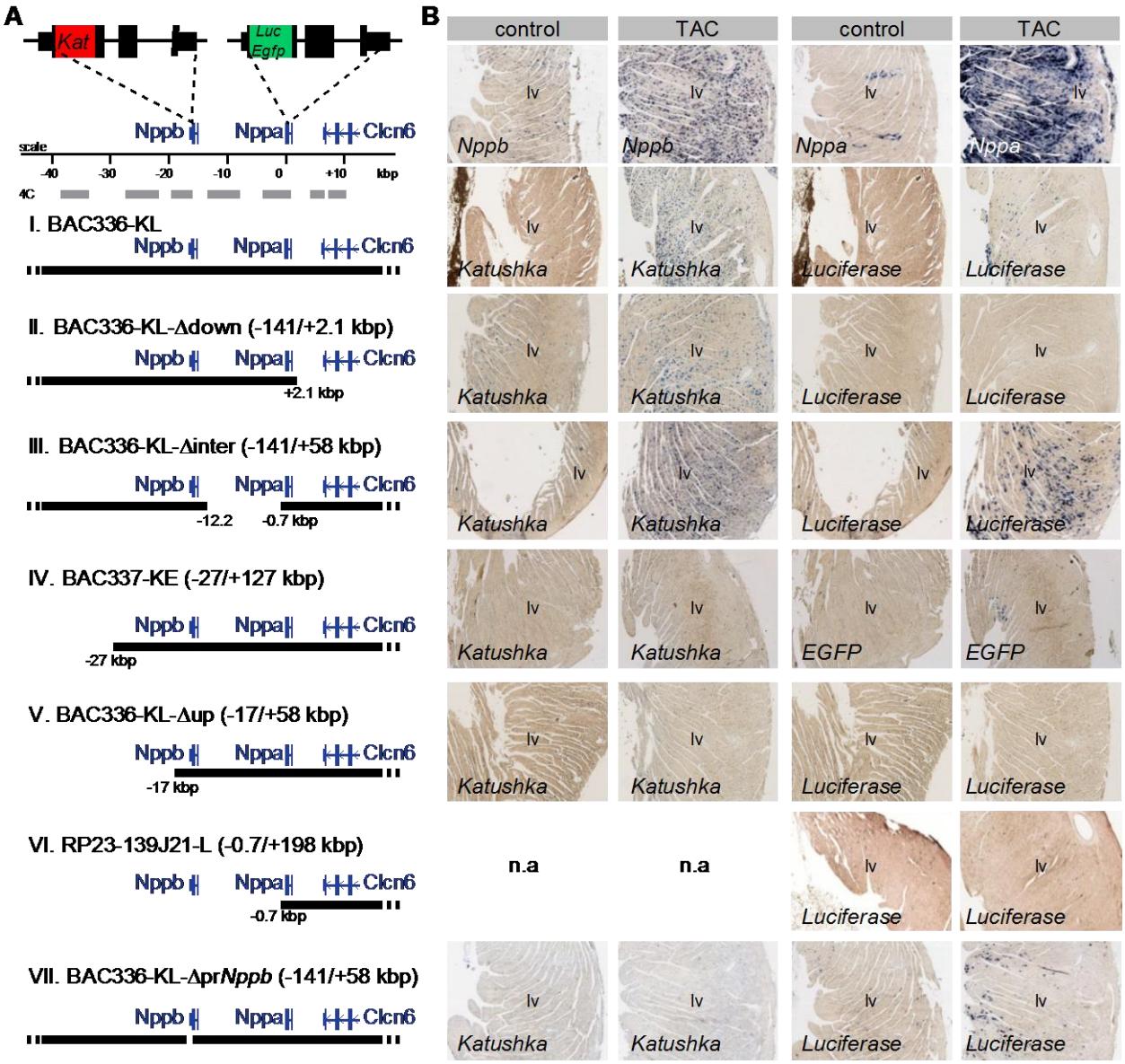

Fig. S4. Overview of the activity of regulatory *Nppa* and *Nppb* sequences during stress. (A) Overview of the overlapping BACs and BAC deletion clones (black lines) with the schematic representation of interacting region (gray lines) as analyzed by 4C-seq. BAC reporter constructs were modified with Katushka and Luciferase/EGFP (KL/E) genes inserted into *Nppb* and *Nppa* translation start sites, respectively (if applicable). (B) Upregulation of *Nppb* and *Nppa* (top raw), and the corresponding *Katushka* and *Luciferase*/*EGFP* genes in the left ventricular myocardium was studied with *in situ* hybridization in the representative TAC hearts compared with the controls.

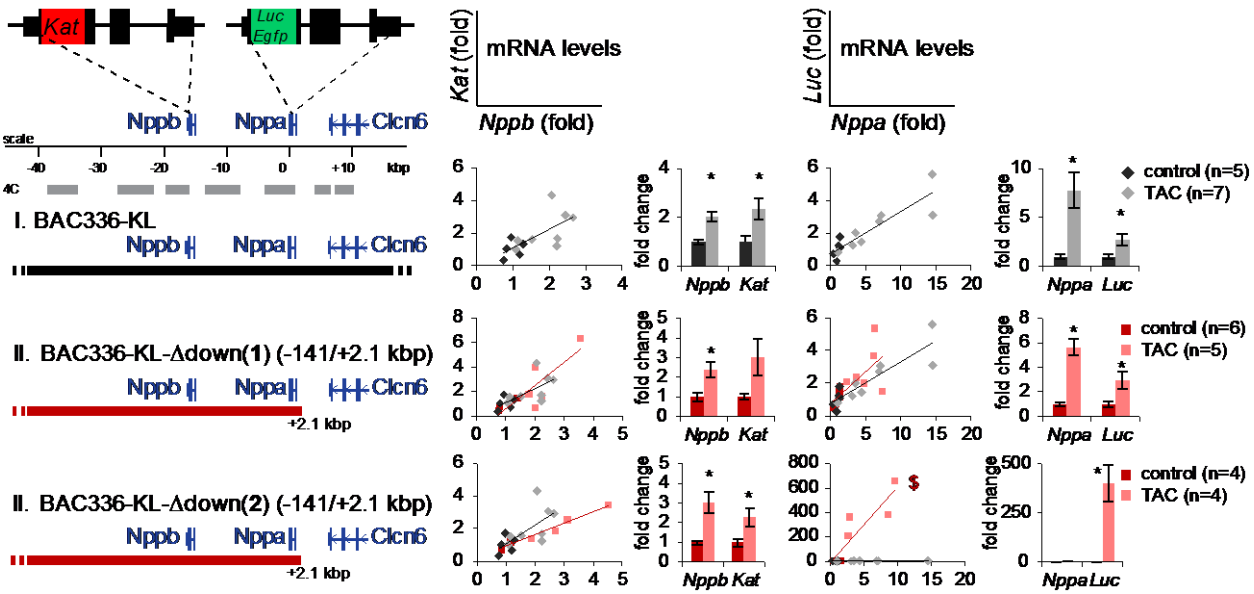

Fig. S5. Two independent founder lines exhibit similar stress-induced activation of the reporter gene expression. BAC336-KL(I) (black line) and BAC336-KL-Δdown(II) (red lines) constructs, and the schematic representation of interacting region (gray lines) as analyzed by 4C-seq are presented in the left panel. BAC reporter constructs were modified with Katushka and Luciferase (KL) genes inserted into *Nppb* and *Nppa* translation start sites, respectively. Correlation of *Nppb* and *Katushka* mRNA levels, and *Nppa* and *Luciferase* mRNA levels in the ventricular myocardium of the control and TAC mice are shown in the 2nd and the 4th columns. Correlation of each pair of genes in the BAC336-KLΔdown (represented in red) was compared with those in BAC336-KL(I) (represented in black), which contains all necessary information for the stress response. Changes in mRNA levels of *Nppb*, *Katushka*, *Nppa* and *Luciferase* are shown in the 3rd and the 5th columns. mRNA levels of the genes were measured by qPCR 2-4 weeks after TAC surgery. *p<0.05 vs. control (Student's two-tailed t-test), § significant vs. BAC336-KL(I) (t-test between the slopes of the regression lines). Error bars represent s.e.m.

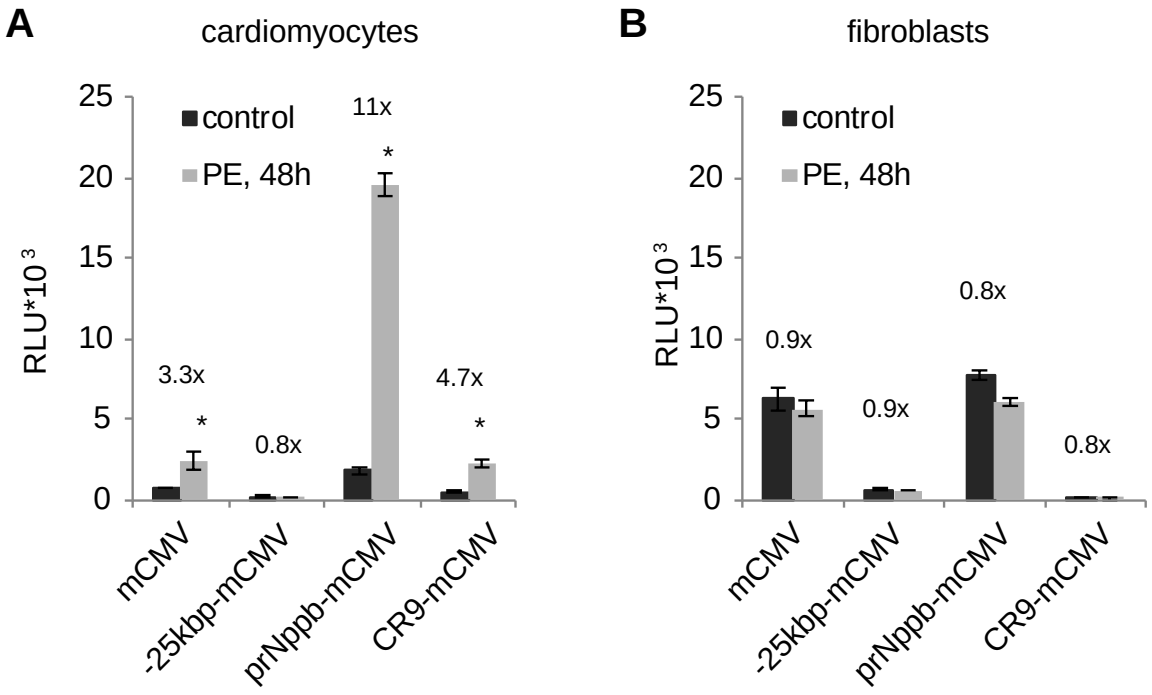

Fig. S6. Identification of enhancer activity of the *Nppb* promoter in response to an α1-adrenergic receptor agonist. Rat neonatal cardiomyocytes (A) and cardiac fibroblasts (B) were treated with PE (100 uM) for 48h. We measured luciferase reporter activities of the minimal CMV promoter (mCMV), the *Nppb* promoter (pr*Nppb*-mCMV), similar size fragment at -25 kbp relative to *Nppa* (-25kbp-mCMV) and the stress-response enhancer CR9 at -37 kbp relative to *Nppa* (CR9-mCMV) used as a positive control (Matsuoka et al., 2014). Numbers above the graphs represent fold activation of Luciferase activity in PE-treated cells compared to control, showing enhancer activity of the *Nppb* promoter and CR9 enhancer specifically in cardiomyocytes. Error bars represent s.e.m. (n = 6 wells in two independent experiments). *P < 0.05 vs. control, Student's two-tailed *t*-test.

construct		Scatter plot Nppb/Kat		Bar charts		Scatter plot Nppa/Lic		Bar charts	
# BAC	Name	Gene correla-tion	2 slopes are different	Nppb	Katush-ka	Gene correla-tion	2 slopes are different	Nppa	Lucife-rase
I(1)	BAC336_KL(TAC)	0.009	n.a	0.002	0.036	4.5E-05	n.a	0.010	0.032
I(2)	BAC336_KL(TAC)	0.023	0.999	0.076	0.102	0.574	0.137	0.095	0.266
I(1)	BAC336_KL(MI)	0.036	n.a	0.157	0.099	0.007	n.a	0.141	0.137
II(1)	BAC336_KL_Δdown	0.009	0.216	0.038	0.095	0.010	0.840	0.001	0.044
II(2)	BAC336_KL_Δdown	4.63E-05	0.221	0.033	0.036	0.002	8.221	0.072	0.023
III	BAC336_KL_ Δinter	4.29E-04	0.059	0.188	0.063	4.68E-04	0.056	0.008	0.005
IV	BAC337_KE	0.823	0.094	0.011	0.618	2.54E-04	4.974	0.011	0.009
V	BAC336_KL_ Δup	0.464	0.065	0.008	0.534	0.336	6.890	0.142	0.856
VI	RP23-139J21_L	n.a.	n.a	n.a.	n.a	0.201	0.001	0.002	0.121
VII	BAC336_KL_ Δ *prNppb*	0.001	0.080	0.190	0.055	0.602	0.004	0.096	0.404
VIII	prNppb-prNppa_L	0.338	0.108	0.304	0.831	0.086	0.048	0.001	0.125

Table S1. P values of the statistical analysis of reporter gene expression in the transgenic mouse lines 2-4 weeks after TAC operation (I-VII) and 1 week after MI (I, VIII), represented in Fig. 4. P values of *Nppa-Luciferase*/*EGFP* and *Nppb-Katushka* correlations on a scatter plot represent the ability of a reporter gene to follow upregulation of *Nppa* or *Nppb,* respectively. Significant slope difference shows that the response of the reporter gene in a given BAC transgenic line is different from that in BAC336-KL(I) mice. P values in a bar chart represent significance of upregulation of *Nppa*, *Nppb* and the reporter gene expression in the ventricles.

Supplementary Materials and Methods

Animals

Animal care and experiments conform to the Directive 2010/63/EU of the European Parliament. All animal work was approved by the Animal Experimental Committee of the Academic Medical Center, Amsterdam (DAE101977, DAE101892, DAE102292, DAE102821), and was carried out in compliance with the Dutch government guidelines. Transgenic mice were generated and bred on the FVB/N background. Genotype of the founder lines and their offspring was analyzed by PCR with tissue-derived (ear, tail, toe, embryo) DNA, and *EGFP* specific (5'Fw- ATCTTCTTCAAGGACGACGG; 5'Rv- AGTTGTACTCCAGCTTGTGC) or *Luciferase* specific primers (5'Fw- ATGTCCGTTCGGTTGGCAGA; 5'Rv- CTGAAATCCCTGGTAATCCGTT) were used.

4C experiment

Preparation of 4C templates was described previously (Simonis et al., 2009). In short, adult mouse hearts and liver were isolated in ice-cold PBS with 10% FCS. Heart tissue was dissociated with IKA Ultra Turrax T5 FU, followed by dounce homogenization to obtain single cell suspension. Liver tissue was homogenized with a douncer only. Chromatin was cross-linked with 2% formaldehyde in 40ml PBS with 10% FCS for 10 min at room temperature, nuclei were isolated in 25ml cold lysis buffer (50 mM Tris-HCl, pH 8.0; 150 mM NaCl; 5 mM EDTA, pH 8.0; 0.5% NP-40; 1% Triton X-100; 1× Protease Inhibitor Cocktail (Roche)) for 1h, and cross-linked DNA was digested with DpnII, recognizing 4-bp restriction site. Digestion was followed by proximity ligation, removal of cross-links, a secondary restriction digestion with Csp6I and a second proximity ligation. For all experiments, 200 ng of the resulting 4C template was used for the subsequent PCR reaction, of which 16 or 8 (total: 3.2 or 1.6 ug of 4C template) were bar-coded, pooled and purified for next generation sequencing. The PCR products were purified using 2 columns per sample of the High Pure PCR Product Purification Kit (Roche), which separates the PCR products larger than 120 bp from the adaptor-containing primers (~75 and ~40 nt).

4C-seq primer design

Detailed rules for 4C primer design were described previously (Werken et al., 2012b). In short, the size of the view point was at least 500 bp to allow efficient cross-linking to other DNA fragments. The region between the primary and secondary restriction enzymes was at least 300 bp to allow efficient circularization during the second ligation step. The reading primer, 20 nt in size, always hybridizes to, and ends at, the 3' side of the first restriction recognition site. The nonreading primers, 18-20 nt in size, were designed at a distance ≤100

bp from the secondary restriction site. 4C primer pairs carry additional 5' overhangs composed of the adapter sequences (obtained from Illumina technical support). The strategy therefore produces sequencing reads (36-mers) composed of the 4C primer sequence (20 nt, specific to a given view point) followed by 16 nt that identify a capture sequence. Primers used in this study are listed below.

primer name	5'-adaptor-**primer**-3'
CTCF left_DpnII	AATGATACGGCGACCACCGAACACTCTTTCCCTACACGACGCT CTTCCGATCT**AAAAGCTCAGAGTGGAGATC**
CTCF left_Csp6I	CAAGCAGAAGACGGCATACGA**ATTCTACTGATGCTGCATGG**
*Nppb*_DpnII	AATGATACGGCGACCACCGAACACTCTTTCCCTACACGACGCT CTTCCGATCT**CAGCTCTCTCTTAGCTGATC**
*Nppb*_Csp6I	CAAGCAGAAGACGGCATACGA**GTGAGCCACATAGCTCCTTC**
*Nppa*_DpnII	AATGATACGGCGACCACCGAACACTCTTTCCCTACACGACGCT CTTCCGATCT**GAGACAGCAAACATCAGATC**
*Nppa*_Csp6I	CAAGCAGAAGACGGCATACGA**TGTCAGGGGCTCCAAATA**
CTCF right_DpnII	AATGATACGGCGACCACCGAACACTCTTTCCCTACACGACGCT CTTCCGATCT**TTCAGTGAGTTCTGGGGATC**
CTCF right_Csp6I	CAAGCAGAAGACGGCATACGA**GTCCTTGCAACAAACAGAAG**

4C-seq data analysis and statistics

4C templates were mixed and sequenced simultaneously in 1 Illumina HiSeq 2000 lane. The sequence tags generated by the procedure were prefixed by the 4C reading primer, which includes the DpnII restriction site sequence (see 4C-seq primer design). The 4C reading primer sequences were separated from multiplexed 4C-seq libraries, and the suffixes were extracted for further processing. Mapping and filtering of the sequence reads was done as previously described (Werken et al., 2012b). The algorithm constructs a background model for remote intra- and interchromosomal contacts to correct for systematic biases that can occur during the 4C-seq experimental protocol. The algorithm is designed to use controls for sequencing errors and nonunique sequences while considering the high coverage (100×–100,000×) of fragment ends that are proximal to the viewpoint fragment. To normalize the interactions in close proximity to the viewpoint, the algorithm was used to calculate the median of normalized coverage for running windows of size 4 kb and sliding windows of 2–50 kb of linearly increasing size. All median values represent enrichment relative to the maximum attainable 4-kb median value, whereas sliding windows represent enrichment relative to the maximum attainable 12-kb median value. The 20th and 80th percentiles were

also computed and depicted as the gray area around the 4-kb running windows. The 4C-seq contact profile comparison plots (Figure 1 C and 2C) were generated combining the mapping (Werken et al., 2012a) and normalization (Werken et al., 2012b) strategies. Within samples the distribution of the blind fragment-end reads and the distribution of the non-blind fragment-end reads were quantile normalized after linear interpolation of the center of the fragment-end using R's limma package (Smyth, 2005). The reads between samples were normalized based on library size within the locus. Subsequently, a running trimmed (10%) mean was calculated on 21 fragment-ends to smoothen the 4C-seq data. The R statistical package version 3.1.0 was used for the statistical calculations and for generating the 4C-Seq plots (R Core Team, 2013).

Chromatin immunoprecipitation

Left ventricles of the control and TAC hearts were dissected in ice-cold PBS, ground in liquid nitrogen and cross-linked in 1% formaldehyde for 10 min at room temperature. Cross-linking was quenched by addition of 0.125M glycine. Tissues were further dissociated by IKA Ultra Turrax T5 FU, pelleted, and resuspended in cold lysis buffer (50 mM Tris-HCl, pH 8.1; 10 mM EDTA, pH 8.0; 1% SDS; 1× Protease Inhibitor Cocktail (Roche); and phosphatase inhibitors: 100 mM PMSF, 54 mM Na-ortho-vanadate, 0.5M Sodium Fluoride, 0.5M β-glycero-phosphate). Nuclei were obtained by use of a tight glass dounce homogenizer. Cross-linked nuclei were sonicated under conditions established to yield an average fragment size of approximately 300 bp. Antibodies were anti-H3K27ac (2 µg, Abcam, ab4729) and anti-Pol II (2 ug, Santa Cruz Biotech, sc-899X). Immunoprecipitation, washing, elution, and reverse cross-linking were performed as previously described (Boogaard et al., 2013). Quality of the ChIP was assessed using the primers on locations of known cardiac enhancers (Boogaard et al., 2012). ChIP-qPCR was performed on a Roche LightCycler 480 System using Sybr Green detection. The ratio of ChIPed DNA normalized for input DNA was compared with that of a negative control region within *Hprt* and is presented as fold enrichment. Control and TAC samples were compared using Student's t-test. Statistical analysis of differences between the region of interest and the negative control region was done with Wilcoxon one-sample test, separately for control and TAC condition. Tested locations were chosen within the *Nppa-Nppb* locus. Primer sequences used in the experiment are listed below.

number	coordinates (mm9)	5'-primer	3'-primer
1	chr4:147327740+147327907	GCTTGAATGTGAATGCCCTC	GGGCTCACATCTCAAACTGC
2	chr4:147331341+147331469	TTGTGACCATTGACCCAGTG	ATACTCTGGATGGGAGATCG
3	chr4:147334441+147334533	GAATGCTGCTACTCTATCTCC	TGTTCAGTGTCATCCAGAGG

4	chr4:147337055+147337151	TCTCTCAGATCCGTCACTTC	AGGTCATAGCCCAAACTCTC
5	chr4:147337649+147337760	ATGATGGCTGGAGGAGGTCT	TTTCGGTGTGGCAAGTTCTG
6	chr4:147337840+147337987	AGGGATAGGAGTGAAACCAG	CGCTTCCTGGGGTCACATT
7	chr4:147339938+147340027	AGCACTTTGCCCGTTCTTTC	ACGTGGAACCCAGAGGAGC
8	chr4:147343583+147343704	AGAACACAGCAGTATGGACG	AACTCTGTCACGTTAGCAGC
9	chr4:147350069+147350184	GGTGTGTGTGTGATGATTAGG	AGCCATTCAAACCCTTGTGC
10	chr4:147353113+147353189	GGGTCACTCTCACTATTCTG	TGAATGTGAGTGACCCCTCC
11	chr4:147353881+147353969	ATTCCGATGTCATTGCTCTCC	CAGAGATGCTGAGTGGCTTAC
12	chr4:147356406+147356568	GTTCAAGCCCAGCCACTAACT	ATAGGCGTGCAGAAATAAGGC
13	chr4:147358867+147359005	TTCTCCATCTCTGCCTTAACC	GAGGAAGTGAAGCTGAGGCAT
14	chr4:147359847+147359958	TGAATACTCCACACAGGCAC	CAGACCTTTTCACGGAGTAG
15	chr4:147360613+147360731	GTTTGGGCTGTAACGGTGAG	GCAGGAGTATGCCAGATAGC
16	chr4:147362077+147362196	CACAATCTCTTCCAAGCCAG	CAGGTGATGGCTCAAATGTG
17	chr4:147363823+147363995	TGCAAGTCAACCTGGTGGAG	ACAACGCTTATGATGGGTGTC
18	chr4:147367710+147367874	CTCAGCAGTCTTTGGTTTCG	AAGGCTTAGTCACTTGGGAG
19	chr4:147373820+147373972	TGTTAAAGGTGGACTGCCTG	GGGACACATACACCATTCTC
20	chr4:147374352+147374444	TAGCTCCAGCATGTGTACTCC	TGTCAGGGGCTCCAAATAAGG
21	chr4:147374890+147374962	AACCAGAGTGGGCAGAGACAG	TGATGGAGAAGGAGCCCATGC
22	chr4:147377093+147377173	ATGTGCGTGTGCCTGTGTA	TACTACTCGGGTTATCCTCC
23	chr4:147378646+147378742	CACCAAGGTCTGCATCAAAC	TGAGATGTCTGCATGTGACC
24	chr4:147382732+147382894	CAGATGAGGGACACTACTTC	CCTTCACCATTTACCGTCTC
25	chr4:147397438+147397598	CCAGACACACTGAACAGCAC	TGGCAGCAGGTTCTGGAATC
Neg(Hprt)	chrX:50361898+50362108	CAACCACTTACTTAGAGGTACT	TTAGCAATATGGACTGTGAGGG
Positive*	chr9:119378854+119379067	TTTGCAGAGGAGGCATGGTG	TCCTCCCTGCAGAAGGGCCT

* Positive control – Scn5a enhancer F9 (Boogaard et al., 2012).

BAC and vector constructs

Generation of BAC336-Katushka-Luciferase (BAC336-KL(I)) and BAC337-EGFP has been described previously (Horsthuis et al., 2008; Sergeeva et al., 2014). In short, BAC modification protocol (Gong et al., 2002) was used to replace the sequences cggcATGgatc and cccacgccagcATGggc at the translation start sites of *Nppb* and *Nppa* (ATG region) with *Katushka* and *Luciferase/EGFP,* respectively. In present study, BAC337EGFP was additionally modified with Katushka (*Nppb*). Using the same protocol (Gong et al., 2002), RP23-139J21(VI) harboring the sequence from -0.65 to +179 kb relative to the transcription start site of *Nppa* was modified with Luciferase (*Nppa*). Also, several truncated BAC336-KL constructs were generated: BAC336-KL-Δdown(II), BAC336-KL-Δpr*Nppb*(VII), BAC336-KL-Δinter(III), BAC336-KL-Δup(V) and BAC336-KL-Δ(-22). In short, two homologous arms (hom) around the targeted regions were amplified with the primers listed below, cloned into the pLD53.SC shuttle vector and used for two consecutive homologous recombination steps in Pir2^{+} bacteria. After both cointegration and resolution, correct recombination was verified by PCR screen using one primer outside a homology arm and another within the

Luciferase/Katushka/EGFP gene. The insertion of the reporter genes and the integrity of the recombinant BAC were confirmed by restriction digest. BAC336-KL(I), RP23-139J21(VI), BAC336-KL-Δ(-22), BAC336-KL-Δdown(II), BAC336-KL-Δpr*Nppb*(VII) DNA was purified using CsCl gradient (Gong et al., 2002). DNA was dialyzed against the injection buffer (10 mM Tris-HCl, pH7.5, 0.1 mM EDTA, 100 mM NaCl, 30 uM Spermine (Sigma), 70 uM Spermidine (Sigma)). BAC337-KE(IV), BAC336-KL-Δinter(III), BAC336-KL-Δup(V) DNA was purified using Nucleobond PC20 Kit (Macherey-Nagel) from the overnight culture. DNA was dialyzed against PBS. An aliquot of purified BAC was checked for degradation via digestion with SpeI and overnight electrophoresis, after which DNA was submitted for pronuclear injection. One or two lines per construct were generated and characterized for fetal and adult expression of the reporter genes.

homol. arm	deleted sequence (chr4)	Fw primer	Rv primer
A(*Nppa*)	cccacgccagcATGggc	CCTGACAGCTGAGCAGCAAG	TCGGGGCACGATCTGATGTT
B(*Nppa*)		TCCTTCTCCATCACCCTG	CCAATCCTGTCAATCCTACC
C(*Nppb*)	cggcATGgatc	TGGTGATGGTGGGTGTTGTTT	CAGAAGCGATGGGCCAGGCA
D(*Nppb*)		TCCTGAAGGTGCTGTCCCAGAT	AAGTGGCAAGGTAGGTGCTCAC
E(Δ(-22))	147,352,566-147,357,560	AGGAGTTTGGGATCAGTGCT	TCAGACTGGTGTCCTTGTGT
F(Δ(-22))		GCCTGTGTCTGTTCTGCCTA	GTGGCTTGGAACTCACTTTG
M(Δinter)	147,362,658-147,374,150	CATAGACACTCTAACCCACTC	CTGTGTAGCCTTGACTATCC
N(Δinter)		TGCTCTTCTAACATCCCTTGG	TCACATTCTTGCTGATTTGCC
O(Δdown)	147,376,982-147,417,481	TTCTGGTTAGAGCCTGGGTG	AGCCCTGAATGTGTTCTCTG
P(Δdown)		TCGGCCATTCTGCCAGAGTT	AAGCCCATTGCAGTTGGTCC
J(Δup)	147,234,647-147,357,560	GTTTCTCTGTGTAGCCCTGG	CCTGGTGTCCTAAACTCATCG
F(Δup)		GCCTGTGTCTGTTCTGCCTA	GTGGCTTGGAACTCACTTTG

To generate EYFP reporter vectors, 5 kb fragments from the *Nppa-Nppb* locus located at -22 kbp and -11 kbp position relative to *Nppa* were amplified from BAC336 (129 SvJ BAC library, Incyte, St Louis, Mo) and cloned into the pGL3basic reporter vector (Promega) modified to contain −638/+70-bp rNppa promoter and EYFP reporter. Primers and genomic coordinates of the putative enhancer regions were:

fragment	Coordinates (mm9)	primers
-22 kbp	chr4:147,352,574-147,357,566	Fw: AGCGGACACCCACATTTATC
		Rv: ACAGGCTGTTAGGTCAGTTG
-11 kbp	chr4:147,362,068-147,366,438	Fw: GTTCTGACCCAGGTTCTC
		Rv: GTCGTGTGATACTTTCCTGAA

Mouse -1.8/+0.28 *Nppb* promoter region (chr4:147358026-147360180) coupled to the bovine growth hormone gene (BGH) poly(A) signal were cloned in reverse orientation

into the pGL3basic-0.7kb*Nppa*-Luciferase reporter downstream Luciferase-polyA sequence. Linearized vector-free constructs were injected in the pronuclei of fertilized eggs, which were subsequently implanted into the oviducts of the FVB preudopregnant foster females to generate transgenic mouse lines.

Transverse aortic constriction

8-12 week-old wild-type or transgenic FVB/N male mice (littermates) were subjected for transverse aortic constriction (TAC) as described (Deel et al., 2011). For 95% confidence interval and the power 0.8, we used 8 animals per TAC group and 4 animals per control group. All mice were weighed, sedated with 4% isoflurane, intubated and connected to a pressure-controlled ventilator (Hugo Sachs Electronic, Harvard Apparatus). A gas mixture of O_2/N_2 (v/v = 1/2) containing 2.5% isoflurane was used to maintain anesthesia. Body temperature was kept at 37˚C and buprenorphine (50 µg/kg) was injected s.c. for postsurgical analgesia. Thoracotomy was performed through the first intercostal space and the aorta was constricted with a 7-0 silk suture, between the truncus brachiocephalicus and the arteria carotis communis sinistra. A 27 G needle was used to induce severe TAC. Age-matched unbanded animals were used as controls. After 4 weeks or if discomfort (dyspnoe, decreasing mobility) was diagnosed earlier, mice were anaesthetized in a CO_2/O_2 mixture, subsequently killed by cervical dislocation and heart tissue was collected. HW/TL ratio was calculated to confirm hypertrophic growth of the hearts. Ventricular apex was used for qPCR and the left ventricle was fixed for 4C and ChIP experiments. Ventricular tissue was dissected and apportioned for qPCR and ISH.

Myocardial infarction

Infarction was created in BAC336KL and pr*Nppb*-pr*Nppa*-Luc mice by permanent ligation of the left anterior descending coronary artery (LAD) according to the protocol described previously (De Celle et al., 2004) with slight modifications. For 95% confidence interval and the power 0.8, we used 12 animals per MI group and 4 animals per control group (taking into account a 65% rate of non-successful experiment, as defined from the experience in the laboratory). Male mice (littermates) mice were sedated with 4% isoflurane, shaved, analgesized subcutaneously with buprenorphine (0.068 mg/kg) and intubated on a heating mat to maintain body temperature. Anesthesia was maintained via ventilation by a Minivent volume controlled Mouse Ventilator (Hugo Sachs Electronic, Harvard Apparatus) with 2% isoflurane in O_2 (1L/min flow rate). Left thoracotomy was performed between the fourth and fifth intercostal space. Infarction was created by permanent ligation of the LAD by surpassing a BV-4 5mm taper point needle with a 9-0 Polyamid wire under the LAD, tied with a double knot. The thoracotomy and skin were closed with a C-1 12mm cutting needle with a 6-0

silicone coated brained silk wire. After 1 week or if discomfort (decreasing mobility) was diagnosed earlier, mice were anaesthetized in a CO_2/O_2 mixture, subsequently killed by cervical dislocation and heart tissue was collected. The border zone of the operated mice and a piece of left ventricles of the control mice were dissected and used for qPCR analysis.

RNA isolation and RT-qPCR

Ventricular tissue of control adult and TAC/MI operated mice was dissected and snap frozen in liquid nitrogen and stored at -80°C. Total RNA was isolated using Trizol Reagent according to the manufacturer's protocol (Invitrogen). 300 ng (fetal tissue) or 500 ng (adult tissue) of total RNA was used for reverse transcription with the Superscript II system (Invitrogen) and Oligo-dT as primers. Expression of different genes was assayed with quantitative real-time PCR using the LightCycler Real-Time PCR system (Roche Diagnostics, Almere, The Netherlands). Target quantities were determined with LinRegPCR and values were normalized to *Gapdh* and *Hprt* expression levels. Primers used:

gene	5'-Fw	5'-Rv
Nppa	TTCCTCGTCTTGGCCTTTTG	CCTCATCTTCTACCGGCATC
Nppb	GTCCAGCAGAGACCTCAAAA	AGGCAGAGTCAGAAACTGGA
Gapdh	GTCAGCAATGCATCCTGCA	CCGTTCAGCTCTGGGATGA
Hprt	TCCTCCTCAGACCGCTTT	CCTGGTTCATCATCGCTAATC
Miip	GAGCAGCATCAGGGTCAAAC	TCTTTTGTCCTGTGAGCTGG
Fv1	CCGCCACAGGATTGAAGTTG	AGTGCCCTCACCTTATCTGC
Mfn2	CTGCTTCAGGATCACCAGTA	GAGAGCAGGAGAGCATGTAG
Plod1	CTGCTTCAGGATCACCAGTA	GAGAGCAGGAGAGCATGTAG
2510039O18Rik	CATCACCCTCTTCCACCTCT	GCTGGGTGTCTTGTGCAAAC
Clcn6	TTCCAGCTCCAGGTCACATC	TCCTGGGAGTTGAAGAAGAG
Mthrf	TCTGGTGACAAGTGGTTCTC	GCCAGGTAACATCTACGAAG
Agtrap	CTTCTCTTGCTGCCTCGTCT	GCAGCGTCTGATGATGAGTC
Nppb in BAC-TG*	AGGGAGAACACGGCATCATTG	TCTCTTATCAGCTCCAGCAG
Luciferase	AGGTGGACATCACTTACGCT	CACTGCATACGACGATTCTG
Katushka	CTTCGACATCCTGGCTACC	TCGTATGTGGTGATCCTCTC
EG/YFP	ATCTTCTTCAAGGACGACGG	AGTTGTACTCCAGCTTGTGC

* Katushka cDNA was inserted in the BAC without its own polyA signal. To prevent miscalculation of the endogenous *Nppb* transcript due to the presence of additional copies of BAC DNA, we used the primers designed in the 5'-UTR and the 2nd exon of *Nppb*.

ISH

Non-radioactive *in situ* hybridization on sections was performed as described previously (Moorman et al., 2001). Embryos and hearts were fixed in 4% formaldehyde, embedded in paraplast and sectioned at 10 µm. The cDNA probes used were *Nppa* (Zeller et al., 1987), *Nppb* (Houweling et al., 2005), *Luciferase*, *Katushka and EYFP.* DIG-labeled *Luciferase* probe was generated from the HindIII linearized pSP-luc+NF vector (Promega) using T7 polymerase. Katushka cDNA was subcloned from pTurboFP-635C (Evrogen) into *pBluescript SK* vector, linearized with EcoRV and labeled with T3 RNA. Images were acquired with the Zeiss Axiophot microscope.

Lentiviral enhancer assay

Lentivirus development

Three fragments were PCR amplified from the mouse BAC336 clone containing the *Nppa* and *Nppb* loci (129 SvJ BAC library, Incyte, St Louis, Mo). The PCR fragments were subcloned into the lentiviral vector encoding the firefly luciferase reporter (pGreenFire Transcriptional Reporter Lentivector; System Biosciences, Mountain View, CA, USA). The lentiviral particles were produced by transfection of 293T cells with the 3 lentiviral packaging plasmids (i.e., pMDLg/pRRE, pRSV-Rev, and pMD2.VSV.G) using polyethylenimine 25 kDa (PEI, Brunschwik) at 1:3 ratio (DNA:PEI). The supernatant from 293T cells containing the lentiviral particles was collected 48 and 72 h after transfection and concentrated by centrifugation in Amicon Ultra-15 Centrifugal Filter Unit (Millipore, UFC910008).

Cardiac myocytes, fibroblasts and luciferase assay

Rat neonatal ventricular myocytes (NRVM) and fibroblasts were isolated from 1-2-day-old Lewis rats, sacrificed by decapitation. Hearts were carefully taken out, atria removed and ventricles cut into small pieces in 1x Hank's balanced salt solution (HBSS, H4641). Ventricular tissue was enzymatically digested using 0.1% trypsin (Affymetrix, 22720) in 1x HBSS over night at 4˚C followed by using 0.1% collagenase I (Invitrogen, 17100-017) in 1x HBSS at 37˚C. Cells were centrifuged, passed through 70 µm cell strainer and pre-plated for 2h in Tung medium (Medium 199 (Invitrogen, 15630-056) supplemented with 10% fetal calf serum (Invitrogen, 26010-074), 10 mM HEPES (Invitrogen. 15630-056), 1x NEAA (Invitrogen 11140-035), 1:100 L-glutamine (Invitrogen, 25030-024), 0,35 g/L D-glucose, 2µg/ml vitamin B12 (Sigma V2876), 1:1000 gentamycin (Invitrogen, 15750-037), 1:100 penicillin/streptomycin (Invitrogen, 15070-063)) to separate myocytes from fibroblasts. After 1 h, cardiomyocytes were collected, counted, and plated at a density of 2,5*105 cells per well in 24-well plates coated with 1% fibronectin (CORNING, 356008). Overnight, NRVM were grown in Tung medium supplemented with 10% fetal calf serum and antibiotics. Fibroblasts were plated at a density $3,3*10^4$ cells per well of in 24-well plates in DMEM

(Invitrogen, 41965-039) supplemented with 10% fetal calf serum (Invitrogen, catalog no. 10270-106) and antibiotics. After 24h, the cardiomyocyte medium was changed to Tung medium without serum (M199 (Invitrogen, 15630-056), 10 mM HEPES (Invitrogen. 15630-056), 1x NEAA (Invitrogen 11140-035), 1:100 L-glutamine (Invitrogen, 25030-024), 0,35 g/L D-glucose, 2ug/ml vitamin B12 (Sigma V2876) and antibiotics). Cardiomyocytes and fibroblast were infected with the lentiviral vectors and the cells were incubated for 16h. Subsequently, the cells were exposed to 100 µM phenylephrine (Sigma, P6126-10G) for 48h. Cell extracts and luciferase assay were performed using *Renilla* Luciferase Assay System according to the protocol (Promega) in the Glomax-Multi detection system.

Statistical analysis of *in vivo* experiments

Direct comparison of *Luciferase* and *Katushka* mRNA levels between different BAC transgenic lines is not possible because the levels of expression in each line depend on the copy-number and the site of integration of the transgenic construct. Therefore, we normalized both fetal and adult ventricular *Luciferase*/*EGFP* and *Katushka* expression levels to that of fetal atrial *Luciferase*/*EGFP* (Figure 2C-D). Fetal atrial expression of *Luciferase/EGFP* was used as a reference because it is provided by the *Nppa* proximal promoter (Habets et al., 2002) present in all the BACs studied. All data in bar charts were represented as mean value ± SEM. The two-tailed Student's t-test was used to determine statistical significance ($p<0.05$) of the differences between the fetal (E17.5) and adult ventricular activity of the reporter genes, and the differences in normalized ventricular activity between different BAC transgenic lines and those of BAC336KL(I).

In TAC and MI experiments, factor correction (Ruijter et al., 2006) was used to remove variability between experiments performed in several sessions. The two-tailed Student's t-test was used to determine statistical significance ($p<0.05$) of genes upregulation. The upregulation of gene expression in the ventricles of TAC mice varied strongly, because of the variable severity of myocardial stress in response to aortic banding. Therefore, we used scatter plots and regression analysis to assess correlations between the levels of endogenous *Nppb* and *Nppa* and their reporters *Katushka* and *Luciferase*/*EGFP*, respectively. Correlation coefficient was used to determine the relationship between the levels of *Nppb* and *Katushka* mRNA, and the levels of *Nppa* and *Luciferase*/*EGFP* mRNA, which represents the response of the reporter genes to stress. T-test between the slopes of the regression lines was used to estimate the difference between the response of the reporter genes in two transgenic lines (Armitage et al., 2008).

References

Armitage, P., Berry, G. and Matthews, J. N. (2008). *Statistical methods in medical research*. John Wiley & Sons.

Boogaard, M. van den, Wong, L. Y., Tessadori, F., Bakker, M. L., Dreizehnter, L. K., Wakker, V., Bezzina, C. R., t Hoen, P. A., Bakkers, J., Barnett, P., et al. (2012). Genetic variation in T-box binding element functionally affects SCN5A/SCN10A enhancer. *J Clin Invest* **122**, 2519–2530.

Boogaard, M. van den, Wong, L. Y., Christoffels, V. M. and Barnett, P. (2013). Acquisition of high quality DNA for massive parallel sequencing by in vivo chromatin immunoprecipitation. *Methods Mol Biol* **977**, 53–64.

De Celle, T., Cleutjens, J. P., Blankesteijn, W. M., Debets, J. J., Smits, J. F. and Janssen, B. J. (2004). Long-term structural and functional consequences of cardiac ischaemia-reperfusion injury in vivo in mice. *Exp Physiol* **89**, 605–615.

Deel, E. D. van, Boer, M. de, Kuster, D. W., Boontje, N. M., Holemans, P., Sipido, K. R., Velden, J. van der and Duncker, D. J. (2011). Exercise training does not improve cardiac function in compensated or decompensated left ventricular hypertrophy induced by aortic stenosis. *J Mol Cell Cardiol* **50**, 1017–1025.

Gong, S., Yang, X. W., Li, C. and Heintz, N. (2002). Highly efficient modification of bacterial artificial chromosomes (BACs) using novel shuttle vectors containing the R6Kgamma origin of replication. *Genome Res* **12**, 1992–1998.

Habets, P. E., Moorman, A. F., Clout, D. E., Roon, M. A. van, Lingbeek, M., Lohuizen, M. van, Campione, M. and Christoffels, V. M. (2002). Cooperative action of Tbx2 and Nkx2.5 inhibits ANF expression in the atrioventricular canal: implications for cardiac chamber formation. *Genes Dev* **16**, 1234–1246.

Horsthuis, T., Houweling, A. C., Habets, P. E., Lange, F. J. de, Azzouzi, H. el, Clout, D. E., Moorman, A. F. and Christoffels, V. M. (2008). Distinct Regulation of Developmental and Heart Disease–Induced Atrial Natriuretic Factor Expression by Two Separate Distal Sequences. *Circulation research* **102**, 849–859.

Houweling, A. C., Somi, S., Massink, M. P., Groenen, M. A., Moorman, A. F. and Christoffels, V. M. (2005). Comparative analysis of the natriuretic peptide precursor gene cluster in vertebrates reveals loss of ANF and retention of CNP-3 in chicken. *Dev Dyn* **233**, 1076–1082.

Matsuoka, K., Asano, Y., Higo, S., Tsukamoto, O., Yan, Y., Yamazaki, S., Matsuzaki, T., Kioka, H., Kato, H., Uno, Y., et al. (2014). Noninvasive and quantitative live imaging reveals a potential stress-responsive enhancer in the failing heart. *FASEB J* **28**, 1870–1879.

Moorman, A. F., Houweling, A. C., Boer, P. A. de and Christoffels, V. M. (2001). Sensitive nonradioactive detection of mRNA in tissue sections: novel application of the whole-mount in situ hybridization protocol. *J Histochem Cytochem* **49**, 1–8.

Ruijter, J. M., Thygesen, H. H., Schoneveld, O. J., Das, A. T., Berkhout, B. and Lamers, W. H. (2006). Factor correction as a tool to eliminate between-session variation in replicate experiments: application to molecular biology and retrovirology. *Retrovirology* **3**, 2–2.

Sergeeva, I. A., Hooijkaas, I. B., Van Der Made, I., Jong, W. M., Creemers, E. E. and Christoffels, V. M. (2014). A transgenic mouse model for the simultaneous monitoring of ANF and BNP gene activity during heart development and disease. *Cardiovasc Res* **101**, 78–86.

Simonis, M., Klous, P., Homminga, I., Galjaard, R. J., Rijkers, E. J., Grosveld, F., Meijerink, J. P. and Laat, W. de (2009). High-resolution identification of balanced and complex chromosomal rearrangements by 4C technology. *Nat Methods* **6**, 837–842.

Stamatoyannopoulos, J. A., Snyder, M., Hardison, R., Ren, B., Gingeras, T., Gilbert, D. M., Groudine, M., Bender, M., Kaul, R., Canfield, T., et al. (2012). An encyclopedia of mouse DNA elements (Mouse ENCODE). *Genome Biol* **13**, 418–418.

Van Keuren, M. L., Gavrilina, G. B., Filipiak, W. E., Zeidler, M. G. and Saunders, T. L. (2009). Generating transgenic mice from bacterial artificial chromosomes: transgenesis efficiency, integration and expression outcomes. *Transgenic Res* **18**, 769–785.

Werken, H. J. van de, Vree, P. J. de, Splinter, E., Holwerda, S. J., Klous, P., Wit, E. de and Laat, W. de (2012a). 4C technology: protocols and data analysis. *Methods Enzymol* **513**, 89–112.

Werken, H. J. van de, Landan, G., Holwerda, S. J., Hoichman, M., Klous, P., Chachik, R., Splinter, E., Valdes-Quezada, C., Oz, Y., Bouwman, B. A., et al. (2012b). Robust 4C-seq data analysis to screen for regulatory DNA interactions. *Nat Methods* **9**, 969–972.

Zeller, R., Bloch, K., Williams, B., Arceci, R. and Seidman, C. (1987). Localized expression of the atrial natriuretic factor gene during cardiac embryogenesis. *Genes & Development* **1**, 693–698.